FINITE ELEMENT SOLUTION OF MHD DUCT FLOWS

by

Osman EGELİ

Submitted to the Faculty of Engineering
in Partial Fulfillment of the
Requirement for the Degree of

Master of Science

in

Mechanical Engineering

Boğaziçi University

Spring 1981

Approved by

Prof. Dr. Akın Tezel	....
Doç. Dr. Fahir Borak	....
Doç. Dr. Muhsin Mengütürk (Thesis supervisor)	....

ACKNOWLEDGEMENTS

I would like to express my gratitude to my thesis supervisor, Doç. Dr. Muhsin Mengütürk for his invaluable comments and discussions during my study. Many thanks for his friendly suggestions and guidance, without him this work wouldn't be possible.

ABSTRACT

In the present study a finite element Galerkin method is presented for the solution of MHD duct flows.

The electromagnetic theory is used to derive the body force term in the Navier - Stokes equation and the ohmic dissipation term in the energy equation. A computer program is set up to solve the finite element formulation of these equations in the case of steady, incompressible, fully - developed flows in ducts with arbitrary cross-section.

In this study, applications to rectangular duct geometries with ideally conducting and insulating boundaries are considered. Comparison of the results provides a good agreement with the other approximate and exact solutions found in the literature. It is observed that in flow of electrically conducting fluids, magnetic field applied in transverse direction retards the flow, inducing electric and magnetic fields in the fluid.

Recommendations towards improvement of the model and for general MHD flow problems are given for future research.

ÖZET

Bu çalışmada MHD kanal akışı çözümleri için bir sonlu elemanlar, Galerkin metodu sunulmaktadır.

Navier - Stokes denklemlerindeki gövde kuvveti ve enerji denklemindeki ohmik yayılma terimleri, elektromanyetik teori kullanılarak elde edilmiştir. Bu denklemlerin sonlu elemanlar ifadeleri, sürekli, sıkıştırılamaz, tümüyle gelişmiş durumlarda, herhangi bir kesite sahip kanallardaki akışlar, geliştirilen kompüter programıyla çözülmüştür.

Bu çalışmada, duvarları mükemmel iletken ve mükemmel izolatör olan dikdörtgen kanal geometrilerine uygulama yapılmıştır. Sonuçların karşılaştırılması literatürdeki diğer çözümlerle iyi bir uyum içinde olduğunu göstermiştir. İletken sıvıların akışında enine uygulanan manyetik alanların akışı yavaşlattığı, akışkanın içinde elektrik ve manyetik alanlar oluşturduğu gözlenmiştir.

Modelin geliştirilmesi ve genel MHD akış problemlerine yönelik gelecekteki araştırmalar için öneriler verilmiştir.

TABLE OF CONTENTS

NOMENCLATURE

a: height of the duct
B: magnetic field
c: specific heat at constant volume.
e: internal energy.
E: electric field.
f: right - hand-side matrix.
h: length of an element.
H: magnetic field strength.
Ha: Hartmann number.
J: current density.
k: stiffness matrix, height to width ratio of the duct.
K: nondimensional electric field.
Ko: permittivity of vacuum.
L: characteristic length of the duct, natural wordinates.
n: unit normal to the boundary.
N: element shape function.
p: pressure field, charge of a single particle.
P: nondimensional pressure gradient.
q": free charge density
Qem: rate of electromagnetic energy
T: temperature field
u: x - component of velocity vector.
u: average velocity.
U: nondimensional velocity.
w: width of the duct.
y : height of the duct.
z : width of the duct.
Δ: area of an element.
u: viscosity.
u: permeability of vacuum.
ξ,η: nondimensional coordinates.
κ: thermal conductivity.
ϕ: conduction parameter.
σ: electrical conductivity.
ρ: density of the fluid.

LIST OF FIGURES

Part I. INTRODUCTION

Magnetohydrodynamics (MHD) can be regarded as the combination of fluid mechanics and electromagnetism with the most essential application in MHD method of electrical power generation which is the direct conversion of thermal energy into electrical energy. Apart from power generation a few examples of applications are:

1. Electromagnetic pumping of liquid metal coolants in nuclear reactors and metallurgical industries.
2. Pumping of propellant gases to obtain high specific impulses for interplanetary flight.
3. Controlled thermonuclear fusion by confining hot ionized deuterium away from walls.
4. Affect the airstream at hypersonic flights for purposes of thermal protection, propulsion or control.
5. Magnetically - controlled lubrication by conducting fluids.

In MHD generators a moving conducting fluid replaces the copper windings in the conventional electrical generators. When this conducting fluid is coused to flow in a duct through a transverse magnetic field, and if electrodes are placed along the sides of the duct, electrical power can be extracted from the system.

The conducting fluid for MHD generation may be a liquid metal or a hot ionized gas. The latter method is more efficient for the conversion of energy in commercial applications.

The basic idea of MHD generation was reported about 1830 by Faraday who performed experiments with moving mercury streams. The first serious attempt at engineering utilization of MHD was made by Karlovitz (1) in the period 1936-1945, while other scientists such as Williams and Hartmann (2) performed simple experiments on the flow of conducting liquids in the laboratory. The emergence of MHD is marked by Alfven (3) who has discovered Alfven waves.

The first large MHD generator is designed and put into operation in 1963 by the Avco-Everett Research Laboratory, known as Avco Mark V, which produced 32 megawatts of electrical power for a few seconds (4).

There has been a continued and determined effort to develop MHD generators for both commercial use and special applications. In the last decade, several scientists and engineers have been investigating performance of MHD generators. Aspnes (5) et al. have simulated an overall MHD steam electrical power generating plant. Sodha (6) has investigated factors affecting power output of an MHD generator and discussed boundary layer effects.

Hara (7) et al have optimized the shape of MHD generator channel in relation to its performance by three - dimensional finite element analysis.

In MHD generators, the problem of duct flow in a transverse magnetic field is of practical interest, yet a difficult analytic problem. It has been formulated by Shercliff (8) in 1953 for two-dimensional fully developed flow. In 1961, Chang (9) has formulated and solved MHD duct flow for a parallel sided duct and a perfectly conducting rectangular duct. The problem of duct flow with arbitrary conductivity is solved by Ihara (10) for circular pipe and by Chu (11) for rectangular ducts. Tani (12) represented an alternative approach based on a variational principle, further he obtained boundary-layer-type solutions by minimization of the variational integral. A wealth of investigations have been carried out to reveal various aspects of MHD flows. Some of the more outstanding of these are mentioned in the following.

Oliver (13) et al, have examined some phenomena of interest in MHD channel flow at high interaction and predicted resulting electrical distributions. Trung (14) studied one-dimensional MHD Faraday generators and indicated general trends in operating characteristics. Miyata (15) has performed experiments on performance of linear Hall MHD generators with high interactions. Gherson (16) et al, have studied analytically the efficiency improvement in liquid metal MHD generators by reduction of the electrical and loses. Asinovskiy (17) et al., have investigated the efficiency obtained in converting the chemical energy of a condensed explosive into electrical energy in a linear explosive MHD generator. Sodha (18) et al., have evaluated the generator performance in the presence of inhomogeneities cdused by growth of ionization instability and velocity/ temperature boundary layer. The effect of boundary layers was also presented by Scheindlin (19) et al., from the experiments performed with argon-potassium plasma. Kirillov (20), Biberman (21) et al., and Zaporowski (22) et al., have treated the heat transfer from plasma to the walls of the generator.

In the present study, one and two-dimensional MHD duct flows are solved numerically by the finite element method. As examples to one-dimensional flows, Hartmann and Couette flows are treated and finite element solutions are compared with exact solutions (23). For the two-dimensional cases, square and rectangular duct flows are solved and are compared with solutions available in literature obtained by other methods such as finite differences (11) and Fourier series (23, 11).

The continuous and discrete formulations of the problems are presented in the second chapter. The third chapter gives a discussion of the results and comparison with available solutions. A detailed derivation of the equations with a review of electromagnetic theory and finite element method and the computer program is given in the appendix.

Part II. DESCRIPTION AND FORMULATION OF PROBLEMS

1. One - dimensional duct flows

The problems considered are the classical examples of MHD flows; steady flow of incompressible, electically conducting fluid with uniform applied magnetic field. Formulations and exact solutions will be given for Hartmann and Couette Flows.
In the first section, the magnetohydrodynamic equations will be formed and nondimensionalized, and in the second section, the equations will be discretized by Galerkin method.

a. Continuous formulation

Consider fully developed fluid flowing in a duct as shown in Fig. 1.

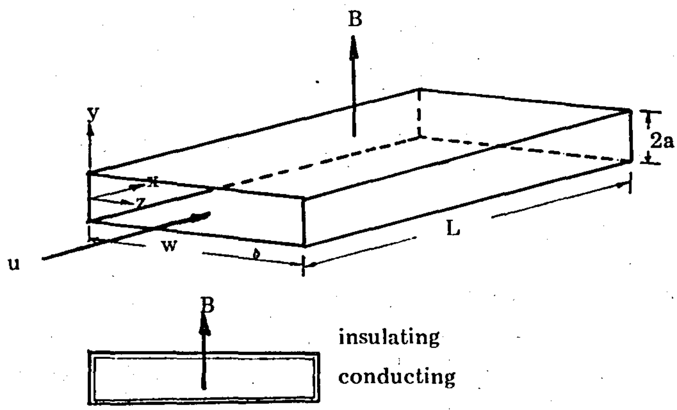

Fig. 1. Channel geometry for 1-D flows

It is further assumed that $W \gg a$ so that there is no variation of any quantities along x and z — axis except pressure.
With the above assumptions. Navier - Stokes equations reduce to (appendix A),

$$0 = -\frac{\partial p}{\partial x} + \mu \frac{d^2 u}{dy^2} - \mu_o H_o J_z \qquad (1.1)$$

$$0 = -\frac{\partial p}{\partial y} + \mu_o H_x J_z$$

$$0 = -\frac{\partial p}{\partial z}$$

Maxwell's equations become:

$$\frac{\partial H_z}{\partial y} = 0 \quad - \quad \frac{\partial H_x}{\partial y} = J_z \quad J_y = 0 \qquad (1.2)$$

$$\frac{\partial E_x}{\partial y} = \frac{\partial E_x}{\partial z} = \frac{\partial E_z}{\partial y} = 0 \qquad (1.3)$$

and ohm's law:

$$J_z = \sigma (E_z + U \mu_o H_o) \qquad (1.4)$$

From y and z components of Eqs (1.1), it can be shown that:

$$\frac{\partial^2 p}{\partial x \partial y} = \frac{\partial^2 p}{\partial x \partial z} = 0$$

therefore, $\partial p/\partial x$ is constant and x-component of Eqs (1.1) are decoupled. Substituion of Eq. (1.4) into Eq (1.1) yields:

$$0 = -\frac{\partial p}{\partial x} + \frac{d^2 u}{dy^2} - \sigma\mu_o (E_z + \mu_o H_o\ U)\ H_o \tag{1.5}$$

This equation can be cast into a nondimensional form by introducing the following variables,

$$U = u/\bar{u} \qquad \eta = y/a \qquad \xi = x/a \tag{1.6}$$

$$Ha^2 = \sigma\mu_o^2 H_o^2 a^2/\mu \qquad K = E_z/\bar{u}B \qquad P = \frac{\partial p}{\partial x}\frac{a^2}{\mu\,\bar{u}}$$

where, Ha is known as the Hartmann number. Thus, Eq (1.5) becomes:

$$\frac{d^2 U}{\partial \eta^2} - Ha^2 U = (P + Ha^2\ K) \tag{1.7}$$

Hartmann and Couette flows differ with boundary conditions. In Hartmann flow, walls are stationary, i.e,

$$U(1) = U(-1) = 0 \tag{1.8}$$

The exact solution to Eq (1.7) with Eq (1-8) is (23);

$$U = \left[\frac{P}{Ha^2} + K\right]\left[\frac{ch\ Ha\eta}{ch\ Ha} - 1\right] \tag{1.9}$$

In Couette flow, the upper wall is moving with a constant velocity Uo as shown in Fig. 2

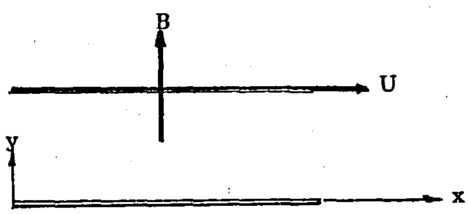

Fig. 2 MHD - Couette flow configuration

Hence, the solution to Eq (1.7) with

$$U(0) = 0 \qquad U(1) = 1 \tag{1.10}$$

is as follows (23);

$$U = -\frac{KHa^2 + P}{Ha^2} + [1 + \frac{2}{Ha^2}(K\,Ha^2 + P)]\,\frac{ch\,Ha\eta}{2ch\,Ha} + \frac{sh\,Ha\eta}{2sh\,Ha} \qquad (1.11)$$

where, $U = u / Uo$

b. Finite Element Formulation

Applying the Galerkin method to Eq. (1.7)

$$\int N_I \left(\frac{d^2 U}{d\eta^2} - U\,Ha^2 + C\right) d\eta = 0 \qquad (1.12)$$

where, $C = -(K\,Ha^2 + P)$

Integrating the second - order term by parts,

$$\int \left(\frac{dN_I}{d\eta}\frac{dU}{d\eta} + Ha^2\,NU - CN\right) d\eta = 0 \qquad (1.13)$$

Substituting the trial function of the form (appendix B);

$$u = \underset{\sim}{N}^T \underset{\sim}{u} \qquad (1.14)$$

the following system of algebraic equations for an element is obtained:

$$[k](u) = (f) \qquad (1.15)$$

Derivation of the equations is given in Appendix C.

2. Two - dimensional Duct Flows

In the few cases of two-dimensional MHD duct flows found in literature, the cross sections considered are rectangular or circular. In this section rectangular duct flows will be treated and the governing equations wili be discretized by Galerkin method. Derivation of the equations can be found in the appendix.

a. Continuous formulation

Consider flow through a rectangular channel as shown in Fig. 3;

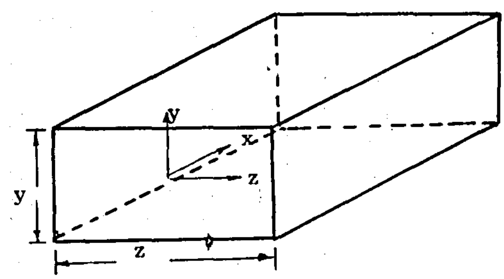

Fig. 3. Two - dimensional flow configuration.

Assuming fully-developed flow, the governing equations are:

Navier - Stokes equations:

$$\begin{aligned} 0 &= -\frac{\partial p}{\partial x} + \mu\left(\frac{\partial^2 u}{\partial y^2} + \frac{\partial^2 u}{\partial z^2}\right) + J_z H_o \mu_o \\ 0 &= -\frac{\partial p}{\partial y} + J_z H_x \mu_o \\ 0 &= -\frac{\partial p}{\partial z} - J_y H_x \mu_o \end{aligned} \tag{2.1}$$

Maxwell's equations;

$$\frac{\partial H_x}{\partial z} = J_y \qquad \frac{\partial H_x}{\partial y} = J_z \qquad \frac{\partial H_y}{\partial z} = 0 \tag{2.2}$$

$$\frac{\partial E_z}{\partial y} = \frac{\partial E_y}{\partial z} \tag{2.3}$$

and Ohm's law:

$$J_y = E_y \sigma \qquad J_z = (E_z + \mu_o u H_o)\sigma \tag{2.4}$$

From Eqs (2.1), it can be shown that $\partial p/\partial x$ is constant. Using Eqs. (2.2).

$$\frac{\partial p}{\partial x} = \mu\left(\frac{\partial^2 u}{\partial y^2} + \frac{\partial^2 u}{\partial z^2}\right) + \mu_o H_o \frac{\partial H_x}{\partial y} \tag{2.5}$$

Eqs (2.2) can be combined to give:

$$\frac{\partial^2 H_x}{\partial y^2} + \frac{\partial^2 H_x}{\partial z^2} + H_o \sigma \frac{\partial u}{\partial y} \mu_o = 0 \tag{2.6}$$

Equations (2.5) and (2.6) can be cast into the following nondimensional forms;

$$\frac{\partial^2 H_x}{\partial y^2} + \frac{\partial^2 H_x}{\partial z^2} + \frac{Ha}{k} \frac{\partial u}{\partial y} = 0 \tag{2.7}$$

$$\frac{\partial^2 u}{\partial y^2} + \frac{\partial^2 u}{\partial z^2} + \frac{Ha}{k} \frac{\partial H_x}{\partial y} = -1 \tag{2.8}$$

where,

$$\begin{aligned} & k = y_o / z_o \quad z = z/z_o \quad y = y/z_o \\ & u = u\mu \left[z_o^2 \left(-\frac{\partial p}{\partial x}\right)\right]^{-1} \\ & H_x = H_x \left[z_o^2 \sqrt{\frac{\sigma}{\mu}} \left(-\frac{\partial p}{\partial x}\right)\right]^{-1} \\ & Ha = H_o y_o \sqrt{\frac{\sigma}{\mu}} \end{aligned} \tag{2.9}$$

Assuming constant wall temperature, energy equation can be written as;

$$\kappa \left(\frac{\partial^2 T}{\partial y^2} + \frac{\partial^2 T}{\partial z^2} \right) + \frac{1}{\sigma} \left[\left(\frac{\partial H_x}{\partial y} \right)^2 + \left(\frac{\partial H_x}{\partial z} \right)^2 \right] + \Phi = 0 \tag{2.10}$$

where,

$$\Phi = \mu \left[\left(\frac{\partial u}{\partial y} \right)^2 + \left(\frac{\partial u}{\partial z} \right)^2 \right]$$

Eq (2.10) can be nondimensionalized as;

$$\frac{\partial^2 T}{\partial y^2} + \frac{\partial^2 T}{\partial z^2} + \left(\frac{\partial H_x}{\partial y} \right)^2 + \left(\frac{\partial H_x}{\partial z} \right)^2 + \left(\frac{\partial u}{\partial y} \right)^2 + \left(\frac{\partial u}{\partial z} \right)^2 = 0 \tag{2.11}$$

with the boundary condition:

$$T = 0 \qquad \text{on } S \tag{2.12}$$

where,

$$T = (T - T_w) \frac{\kappa \mu}{\left[z_o^2 \left(-\frac{\partial p}{\partial x} \right)^2 \right]^2}$$

The most general boundary condition on the magnetic field is [11];

$$\frac{\partial H_x}{\partial n} + \phi H_x = 0 \qquad \text{on } S \tag{2.13}$$

where, ϕ is the conduction parameter defined as the ratio of fluid conductivity to the wall conductivity. For the extreme cases, i.e;

Perfectly conducting walls: $\phi \to 0$

$$\frac{\partial H_x}{\partial n} = 0 \qquad \text{on } S \tag{2.14}$$

Perfectly insulating walls; $\phi \to \infty$

$$H_x = 0 \qquad \text{on } S \tag{2.15}$$

The system of partial differential equations, Eq (2.7) and Eq (2.8) are solved with Eq (2.13) and the no-slip boundary condition;

$$u = 0 \qquad \text{on } S \tag{2.16}$$

b. Finite Element Formulation

Applying Galerkin method to Eqs (2.7) and (2.8),

$$\iint N_i \left[\frac{\partial^2 H_x}{\partial y^2} + \frac{\partial^2 H_x}{\partial z^2} + \frac{Ha}{k} \frac{\partial u}{\partial y} \right] dydz = 0 \tag{2.17}$$

$$\iint N_i \left[\frac{\partial^2 u}{\partial y^2} + \frac{\partial^2 u}{\partial z^2} + \frac{Ha}{k} \frac{\partial H_x}{\partial y} + 1 \right] dydz = 0 \tag{2.18}$$

The second-order terms impose unnecessary continuity requirements. Thus, using Green's theorem, Eqs (2.17) and (2.18) become;

$$\iint \left(\frac{\partial N_i}{\partial y} \frac{\partial H_x}{\partial y} + \frac{\partial N_i}{\partial z} \frac{\partial H_x}{\partial z} - \frac{Ha}{k} N_i \frac{\partial u}{\partial y} \right) dydz - \int N_i \frac{\partial H_x}{\partial n} ds = 0 \tag{2.19}$$

$$\iint \left(\frac{\partial N_i}{\partial y} \frac{\partial u}{\partial y} + \frac{\partial N_i}{\partial z} \frac{\partial u}{\partial z} - \frac{Ha}{k} N_i \frac{\partial H_x}{\partial y} - N_i \right) dydz - \int N_i \frac{\partial u}{\partial n} ds = 0 \tag{2.20}$$

Eqs (2.19) and (2.20) can be written for every node i. It should be noted that the surface integrals do not contribute anything to the governing equation at the internal nodes. When the node i lies on the boundary, then the surface integrals will be treated according to the physical boundary conditions:

case 1: If nodal values of u and H are prescribed at node i, then ith equation in (2.19) and (2.20) are not formed, therefore, the surface integrals are not needed.

case 2: If the normal derivatives of H are given at node i, then the surface integrals will be evaluated in Eqs (2.19) and (2.20).

For the two cases, from Eqs (2.11), (2.12) and (2.13), the surface integrals will not be needed. Using a trial function of the form;

$$H_x = N H_j \qquad u = N \mu_j \tag{2.21}$$

Eqs (2.19) and (2.20) become;

$$\begin{aligned} &[k]\,(H) + [k]\,(u) = 0 \\ &[k]\,(H) + [k]\,(u) = (f) \end{aligned} \tag{2.22}$$

The evaluation of the integrals to form element equations are given in Appendix C.

Applying the same procedure to energy equation, Eq (2.11) becomes,

$$\iint \left(\frac{\partial N_i}{\partial y} \frac{\partial T}{\partial y} + \frac{\partial N_i}{\partial z} \frac{\partial T}{\partial z} - N_i [\nabla H \nabla H + \nabla u \nabla u] \right) dydz - \int N_i \frac{\partial T}{\partial n} ds = 0 \tag{2.23}$$

Since the wall temperatures are prescribed, the surface integrals will not be needed. Using Eqs (2.21) with,

$$T = N T_j \tag{2.24}$$

Equation (2.23) can be written as;

$$[k]\,(T) = (r) \tag{2.25}$$

where

$$(r) = \iint N_i [\; H^T \nabla N_j^T \nabla N_j \; H + u^T \nabla N_j^T \nabla N_j \; u] \; dydz \tag{2.26}$$

Since the energy equation is decoupled from equation of motion, Eq (2.25) can be solved seperately from Eq (2.24) with the known values of u and H.

Part III. RESULTS and DISCUSSION

1. One - dimensional duct flows

One - dimensional Couette and Hartmann flows have been solved for various Hartmann numbers.

Fig. 4 shows the calculated velocity profiles of the Hartmann flow for various values of Ha. These profiles are constructed by using nondimensional parameters. The nondimensional velocity is expressed in terms of a normalized velocity as u/f (Ha, K, P), where f(Ha, K, P) is a function of Hartmann number, pressure gradient and the parameter K, given by Eq (1.12).

Each profile indicates an excellent agreement between the present finite element solution and the exact solution [23]

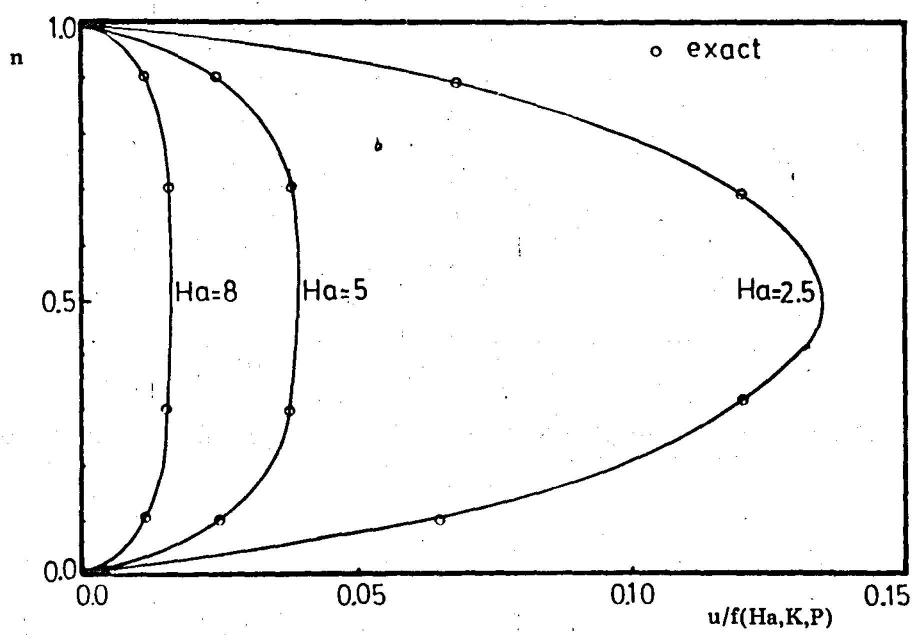

Fig. 4. Normalized velocity profiles for Hartmann flow, as calculated by the present method and the exact solution [26].

The slowing effect of Ha can be easily observed. This is due to the fact that in flow of conducting fluids through transverse magnetic field, electromagnetic body force will act in the opposing direction and retard the flow.

Figs. 5 and 6 show the velocity profiles of the Couette flow for various values of Ha with zero pressure gradient and with different values of the parameter K, corresponding respectively to short and open-circuited cases.

The results are in good agreement with the exact solution as in Fig. 4.

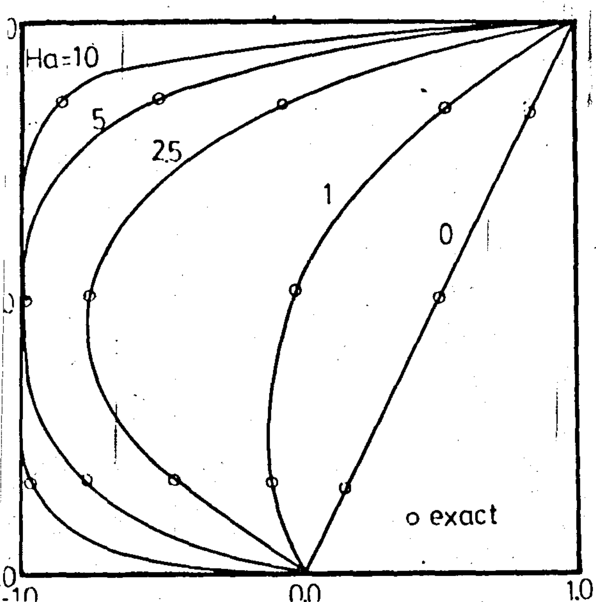

Fig. 5. Velocity profiles for Couette flow with the parameters P:0, K:1.

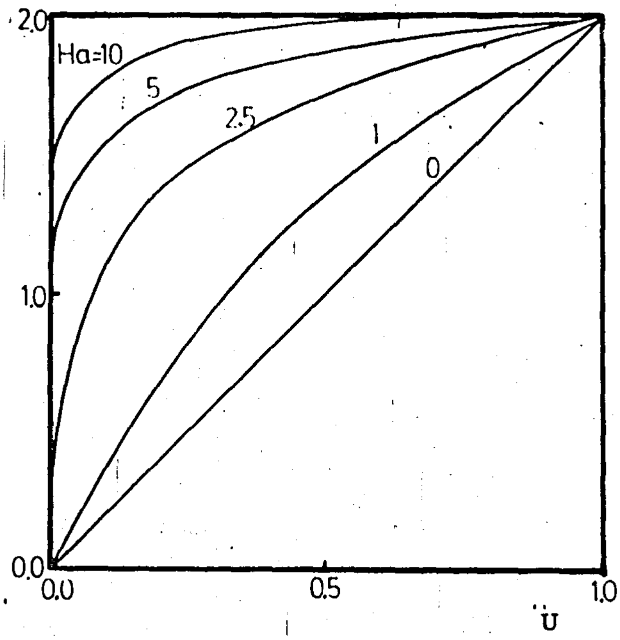

Fig. 6. Velocity profiles for Couette flow with the parameters P:0, K:0.

The slowing effect of Ha is again apparent in both cases, but the profiles corresponding to K=1 appear to be more sensitive to Ha.

Fig. 7 shows the calculated flowrate of the Hartmann flow as a function of Ha. The nondimensional flowrate is normalized with the flowrate at Ha=0. It is noted that flowrate decreases very rapidly until Ha≅5 and drops to negligible proportions for Ha>10.

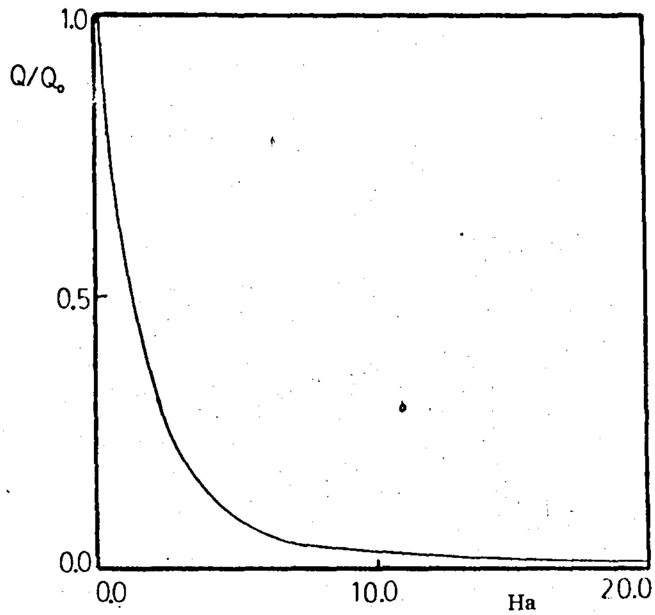

Fig. 7. Normalized flowrate versus Hartmann number. Q_0 is the flowrate at zero Ha.

2. Two-dimensional duct flows

Results have been obtained for square and rectangular ducts with perfectly conducting and perfectly insulating walls for various values of Ha.

Figs. 8 and 9 show the nondimensional velocity contours and profiles at certain cross-sections of the duct at zero Hartmann number, for square and rectangular ducts, respectively. It can be seen that velocity is maximum at the center and decreases towards the walls.

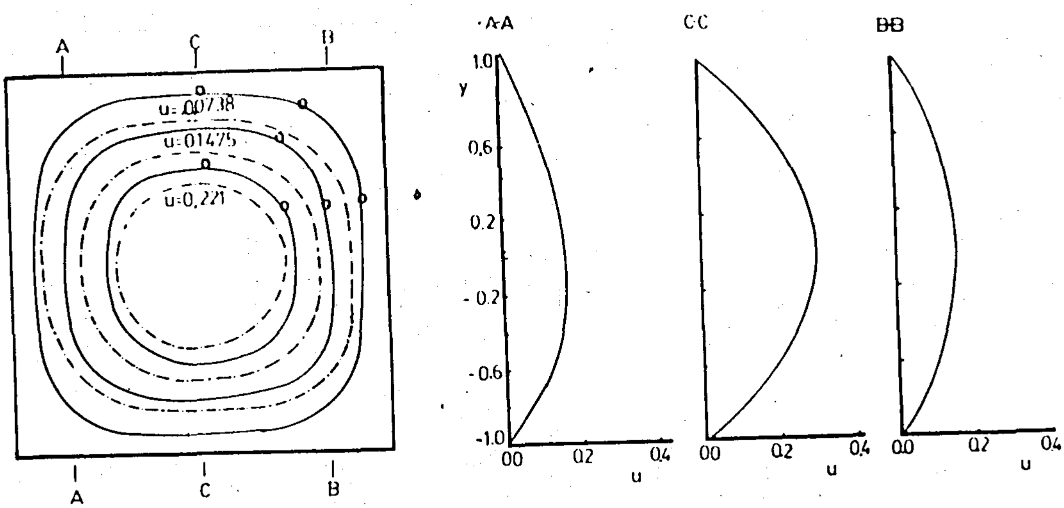

Fig. 8. (a) Velocity contours for square duct calculated by the present method and the fourier series [23] at Ha:0 for different mesh sizes.

(b) Velocity profiles at certain cross sections of the duct at Ha:0.

— n : 200
— — ne : 128
—.— n : 32
o fourier series solution.

There is a good agreement between the present finite element solution and the fourier series solution [26], the error decreasing with decreasing mesh size, shown in Fig. 8 (a). This is also illustrated in Fig. 10, in which the relative error in the maximum velocity is plotted versus total number of nodes. It is seen that there is a rapid convergence to the exact solution with increase in the number of nodes.

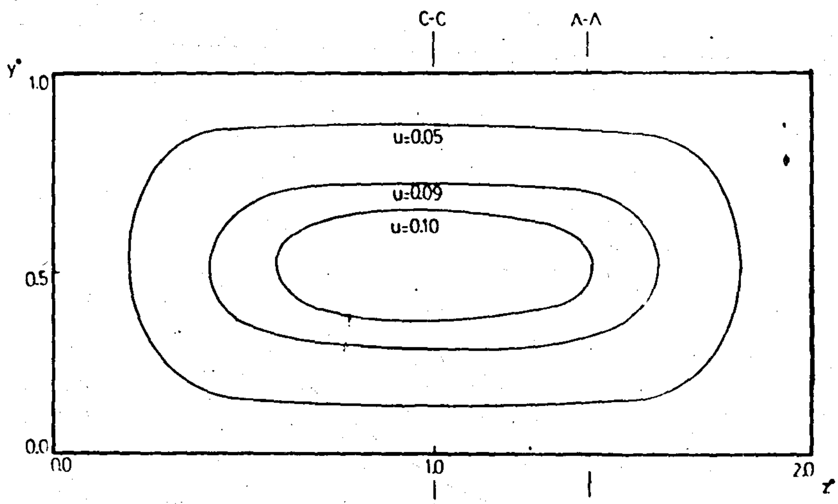

Fig. 9. (a) Velocity contours for rectangular duct.

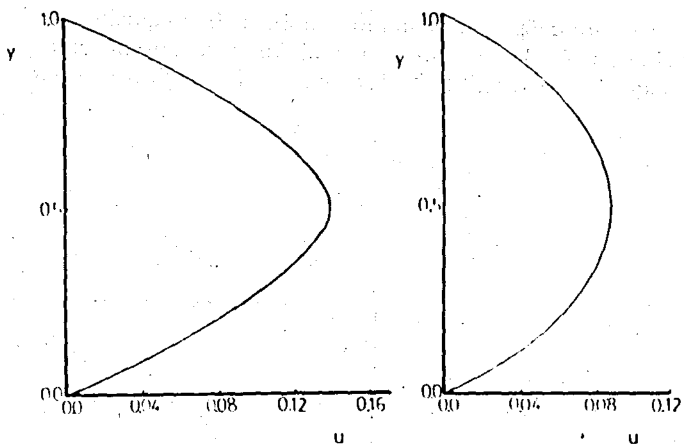

(b) Velocity profile at the certain cross sections.

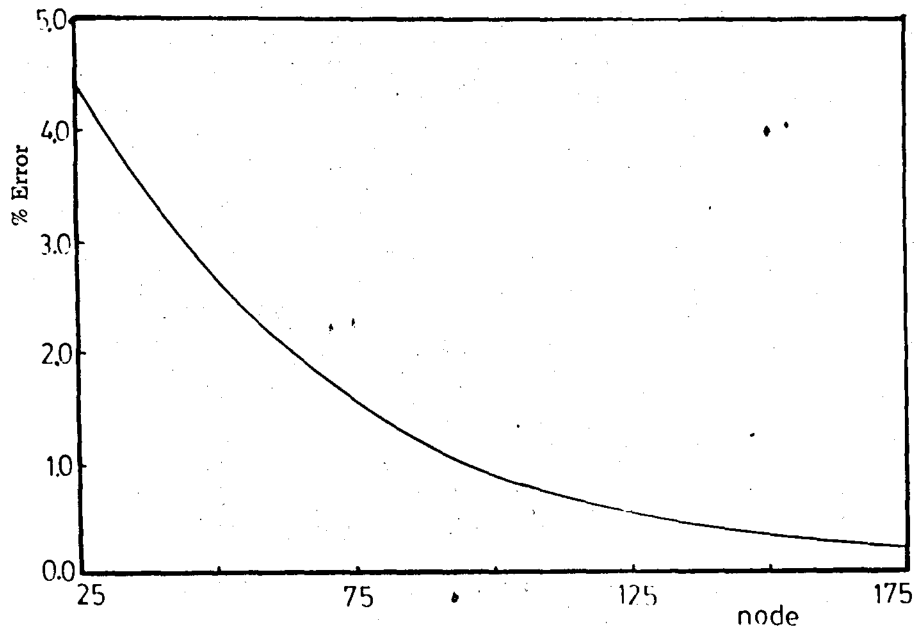

Fig. 10. Relative error in maximum velocity versus number of nodes.

Fig. 11 shows the calculated nondimensional contours and profiles for square duct at Ha=0. Due to symmetry of the contours, only one quadrant of the duct is shown. The figure indicates that maximum temperature occurs at the center of the duct which is due to the fact that viscous dissipation is maximum at the centerline.

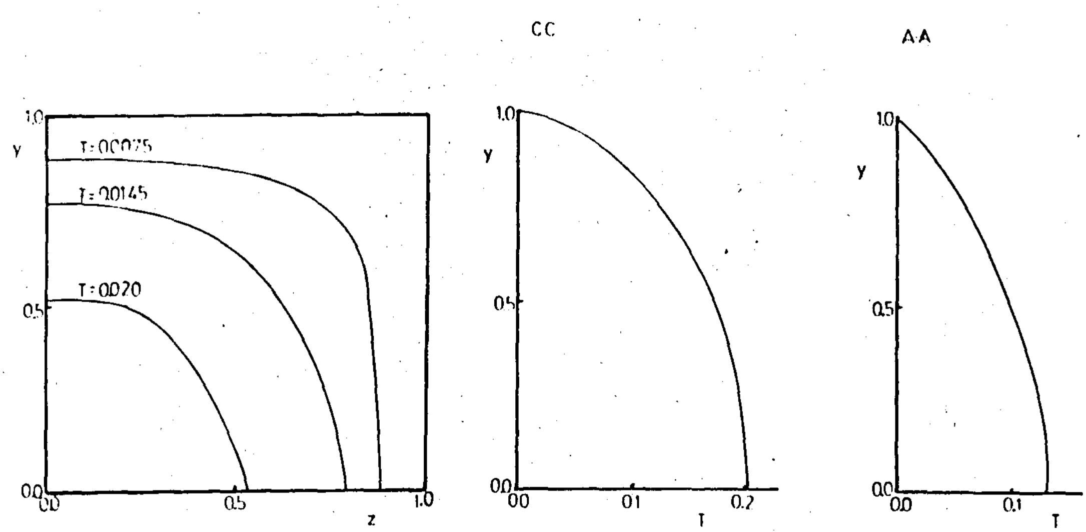

Fig. 11. (a) Temperature contours at zero Ha.

Results for nonzero Hartmann numbers are presented in two categories corresponding to the extreme cases of perfectly conducting and insulating boundaries.

i. Perfectly conducting walls:

Figs. 12 and 13 show the velocity contours in one quadrant of the duct at Ha =0.001 for square and rectangular ducts, respectively. Since the contours are symmetric, only one quadrant of the duct is shown. Also shown in these figures are the contours for Ha=0 as copied from Figs. 8 and 9. Comparison of profile shapes indicates that MHD distortion of velocity profile is negligible at very small Hartmann numbers.

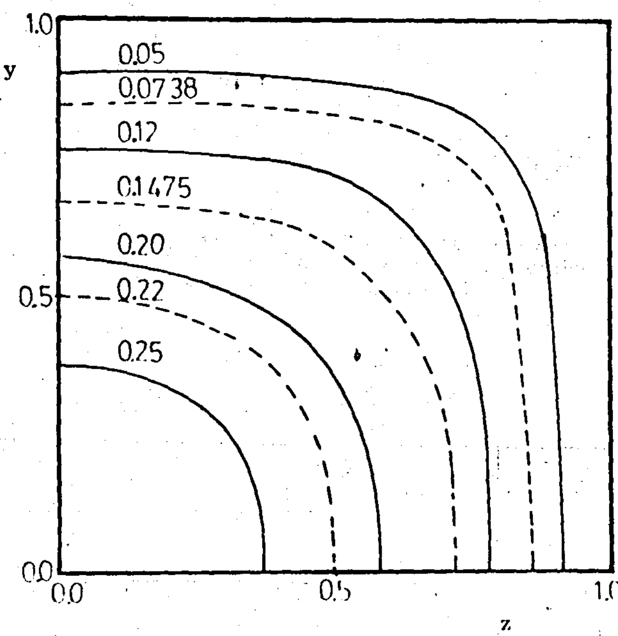

Fig. 12. Velocity contours for perfectly conducting square duct at Ha: 0.001. Dashed lines are contours at Ha: 0.

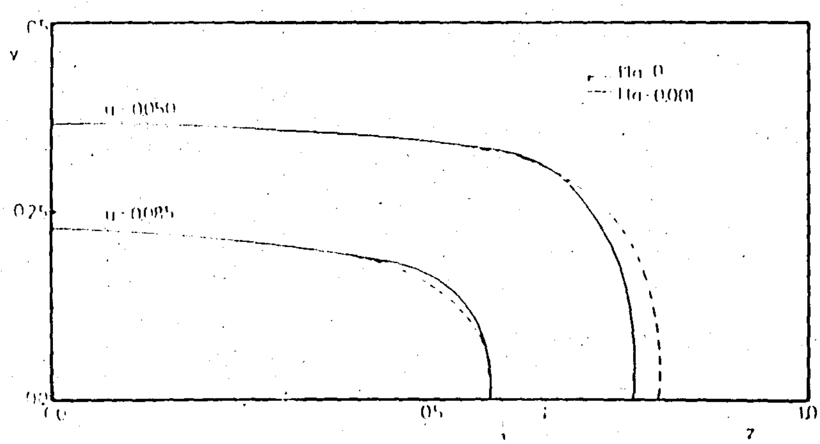

Fig. 13. Velocity contours for perfectly conducting rectangular duct.

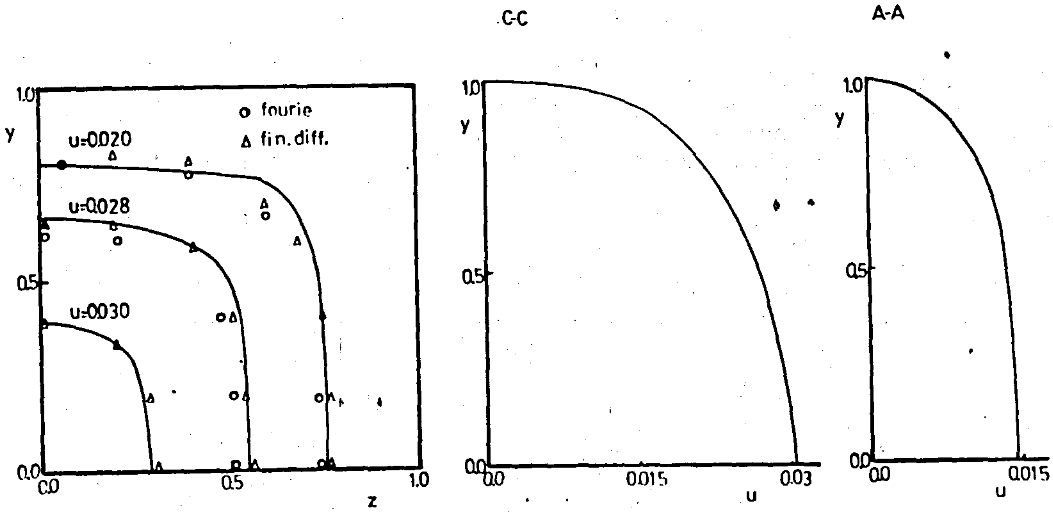

Fig. 14. (a) Velocity contours for perfectly conducting square duct at Ha: 6 as calculated by the present method finite differences and Fouries series [11].
(b) Velocity profiles at certain cross sections.

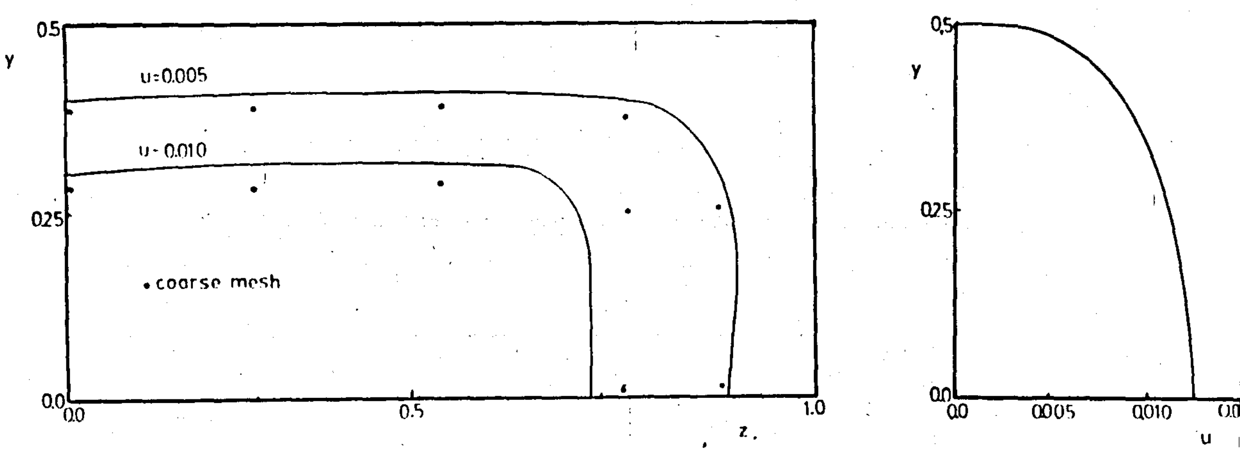

Fig. 15. (a) Velocity contours for perfectly conducting rectangular duct at Ha:5.
(b) Velocity profiles at certain cross sections.

Figs. 14 and 15 show the calculated velocity contours and profiles at Ha=6 and 5, for square and rectangular ducts respectively. Fig. 14 (a) indicates a good agreement between the present finite element solution and other solutions by the Fourier series and the finite difference methods [11].

Comparison of Figures 14 (b) and 15 (b), respectively, with Figs. 8 (b) and 9 (b) illustrates the extend by which flow is retarded and profiles are flattened with increase in Ha.

Figs. 16 and 17 show the nondimensional induced magnetic field lines for square and rectangular ducts. It is seen that the constant magnetic field lines which are the current lines extend all the way to the walls of the duct due to the fact that the walls perfectly conducting, so that the current flows through the fluid and returns from the walls. The present solution is again in good agreement with finite difference solution [11] shown in Fig. 16.

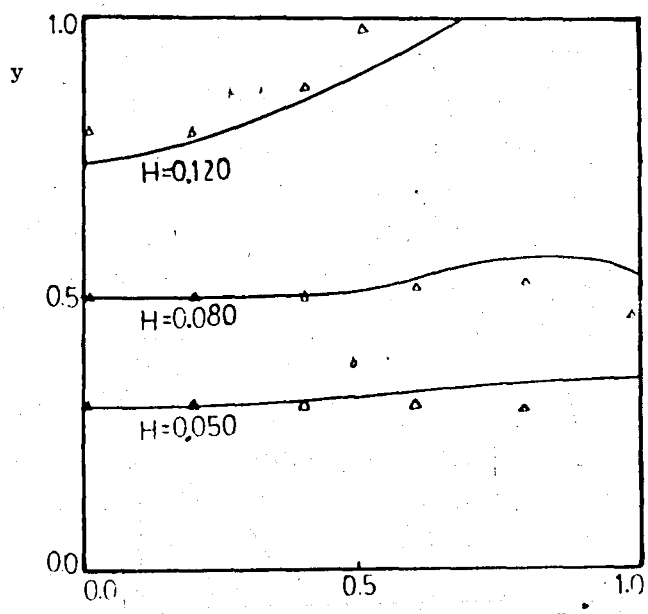

Fig. 16. Constant induced magnetic lines at Ha:6 for perfectly conducting square duct.

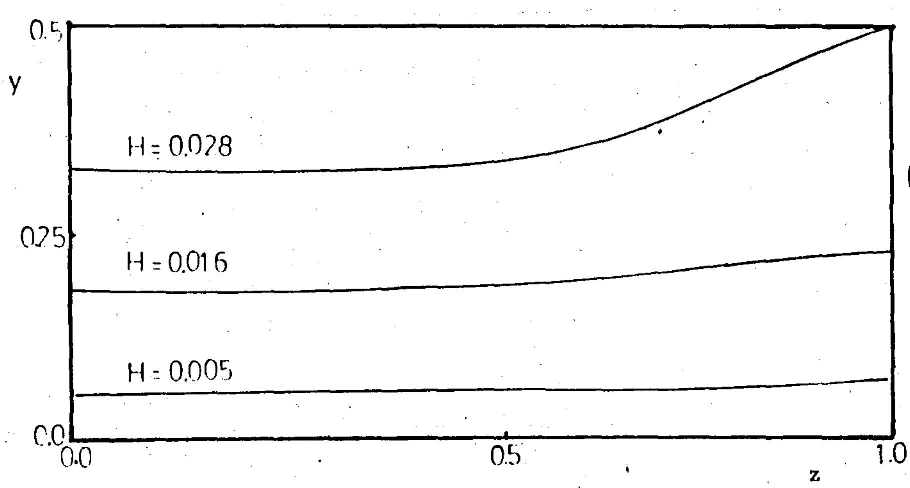

Fig.17. Constant induced magnetic field lines at Ha:5 for perfectly conducting rectangular duct.

Figs. 18 and 19 show the calculated temperature contours at Ha=6 for one quadrant of square and rectangular ducts. The maximum temperature still lies on the centerline of the duct and decreases towards the walls. The figures indicate a decrease in temperatures in comparison to values at Ha = 0 (Fig.11). This is due to the fact that viscous dissipation is dominant over the ohmic dissipation for reasonable values of Ha and it decreases as the flow is retarded.

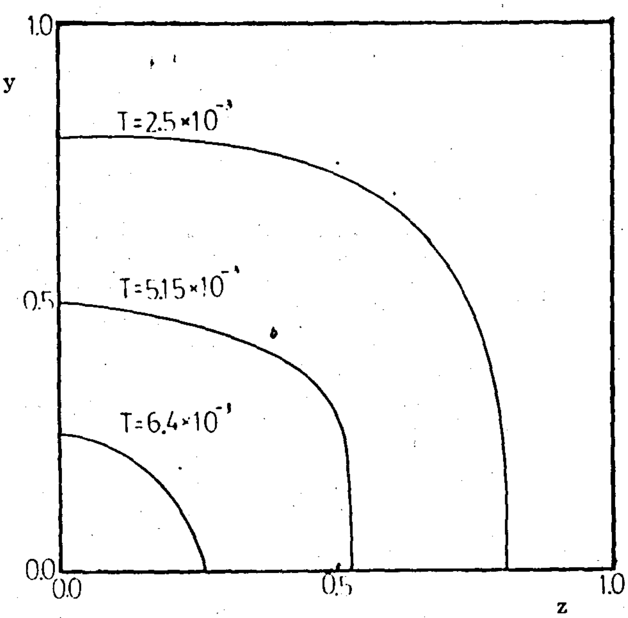

Fig. 18. Temperature contours at Ha:6 for perfectly conducting square duct.

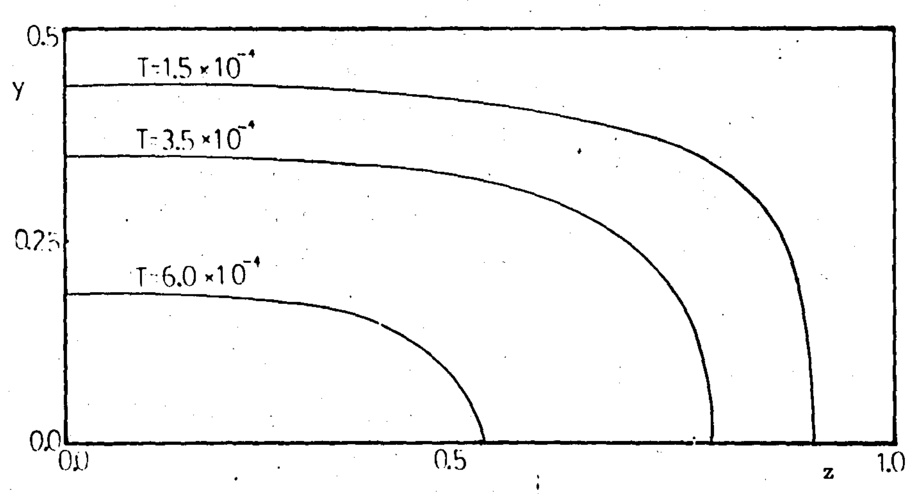

Fig. 19. Temperature contours at Ha:6 for perfectly conducting rectangular duct.

(ii) Perfectly insulating walls:

Fig. 20 shows the calculated nondimensional velocity contours at Ha = 5 for square duct. Since the walls are now perfectly insulating, the velocity field is less affected by the magnetic field than in the case of conducting walls. This can be seen by comparing Fig. 20 with Fig. 14. The figure also indicates a good agreement between present solution and Fourier series solution [26].

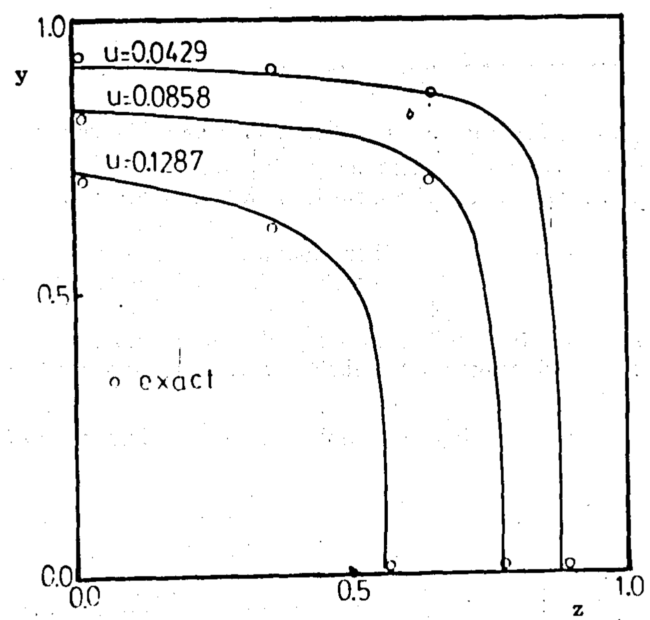

Fig. 20. Velocity contours at Ha:5 for perfectly insulating square duct as calculated by the present method and the method of Fourier series. [23].

Perfectly insulating walls cause current lines to from close loops in fluid.

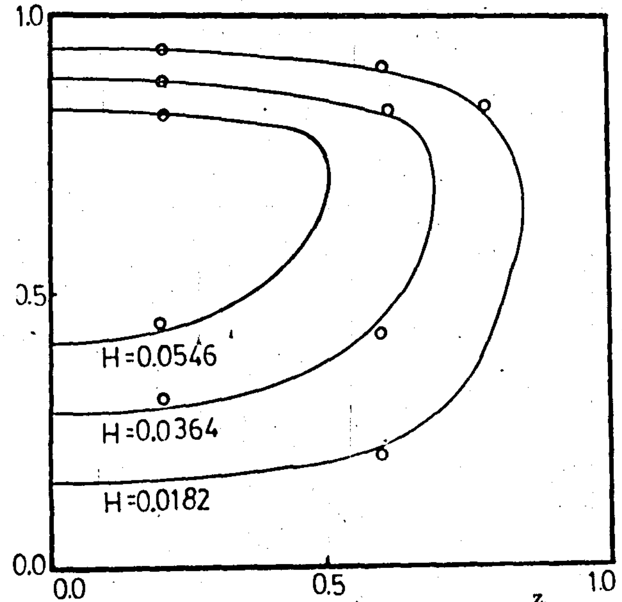

Fig. 21. Induced magnetic field contours at Ha:5 for perfectly insulating square duct.

Fig. 21 shows the constant induced magnetic field lines at Ha = 5 for square duct. The contours indicate a good agreement between present finite element solution and the Fourier series solution.

Fig. 22 shows the temperature contours at Ha = 6 for square duct. Comparison with Fig. 18 reveals that the profiles are less affected in insulated duct.

In Fig. 23, temperature profiles along the centerline of the square duct is shown for various values of Ha. Flattening of the profiles for increasing Ha is due to decrease in viscous dissipation.

Comparison of the results for perfectly insulating and perfectly conducting walls is given in Figs. 24 through 29.

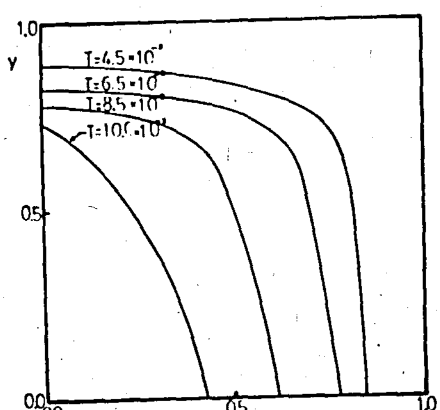

Fig. 22. Temperature contours at Ha:6 for perfectly insulating square duct.

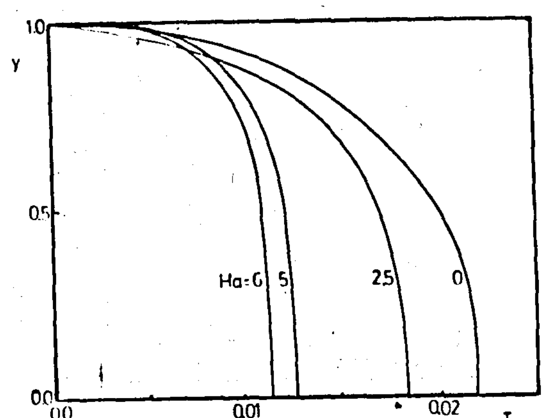

Fig. 23. Temperature profiles along the centerline of the perfectly insulating square duct for various values of Ha.

Figs. 24 and 25 show the calculated velocity profiles along the centerline of the channel for various values of Ha, for square and rectangular ducts, respectively. It is observed that electromagnetic field exerts a greater effect in the case with conducting walls.

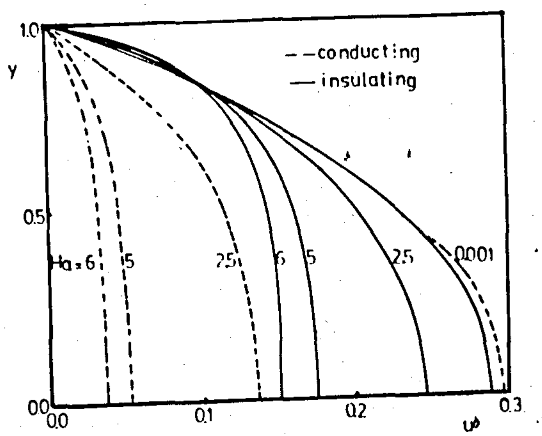

Fig. 24. Velocity profiles along centerline of the square duct.

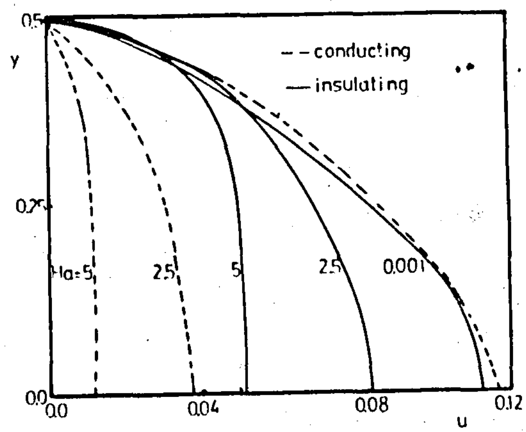

Fig. 25. Velocity profiles along centerline of the rectangular duct.

Fig. 26 shows the calculated maximum velocity versus Hartmann number in square duct. Results with mixed boundaries, i.e. perfectly insulating walls parallel to the magnetic field and perfectly conducting wall perpendicular to it are also shown for comparison. It is seen that there is a rapid decrease in maximum velocity for increasing values of Ha.

Fig. 27 shows the maximum velocities for rectangular duct for the perfectly insulating, perfectly conducting and mixed boundaries as in the above. It is observed that the velocities are more readily affected than in square duct. The figure also shows that the conductivity of the side walls has negligible effect on the maximum velocity unlike the square duct (Fig. 26).

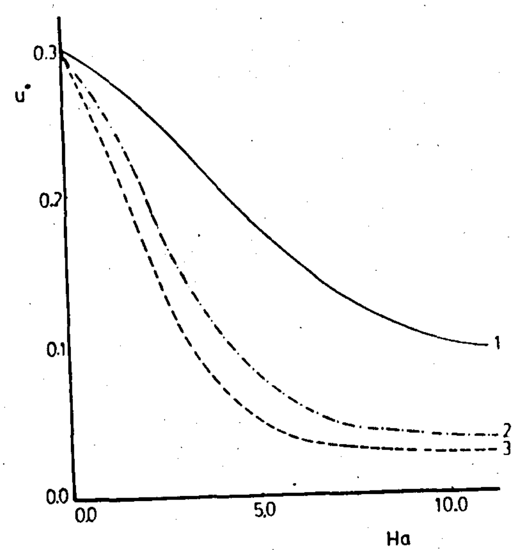

Fig. 26. Maximum velocity in the square duct ~~versus Hartmann~~ number for 1. perfectly insulating, 2. perfectly conducting walls perpendicular to applied magnetic field, 3. perfectly conducting walls.

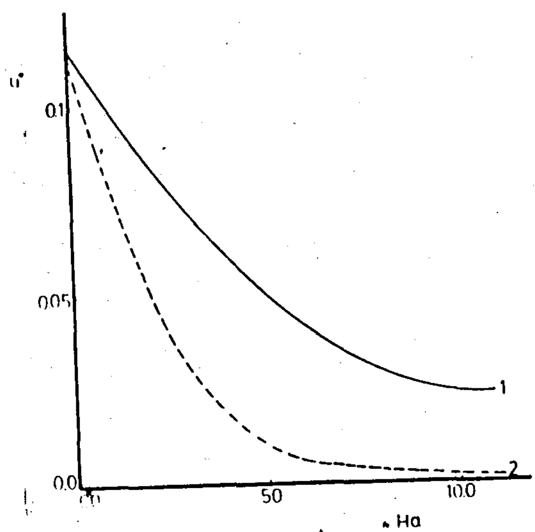

Fig. 27. Maximum velocity in rectangular duct versus Hartmann number for: 1. perfectly insulating ; 2. perfectly conducting walls.

Fig. 28 shows the calculated maximum temperature versus Hartmann number in square duct for perfectly insulating and perfectly conducting walls. The profiles are constructed by using temperatures normalized by the maximum temperature at Ha = 0.

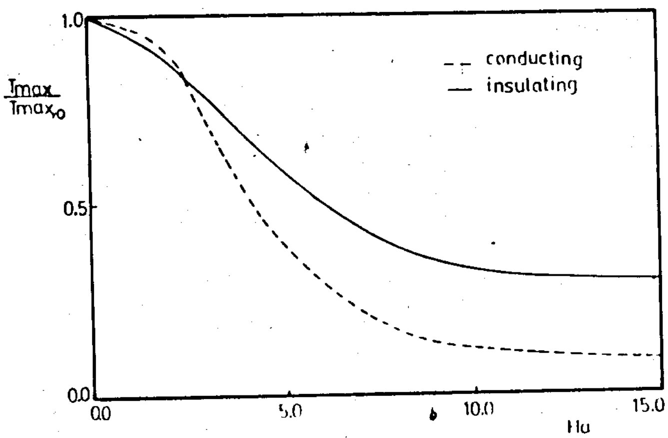

Fig. 28. Normalized maximum temperature versus Hartmann number for square duct.

Fig. 29 shows the flowrate normalized with the value at zero Ha, as a function of Hartmann number.

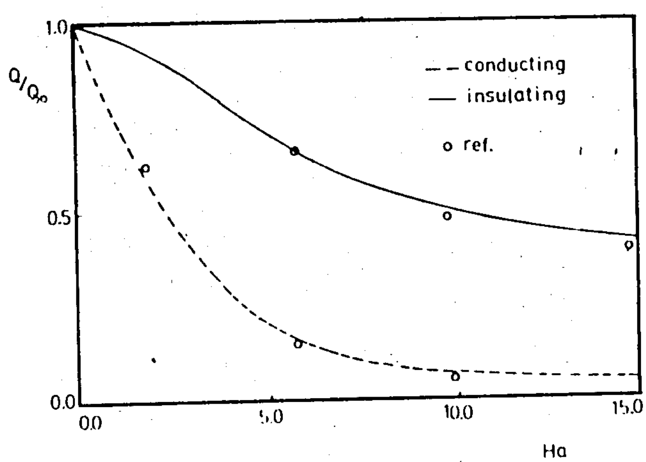

Fig. 29. Normalized flowrate versus Hartmann number for square duct as calculated by the present method and the method of Fourier series.

Part IV. CONCLUSIONS and RECOMMENDATIONS

A computer program has been developed to solve MHD duct flows by the finite element method.

The applicability of the model has been shown by solving a few example problems, the results being in good agreement with other exact and approximate solutions.

The problems considered were one and two - dimensional fully developed duct flows under transverse magnetic fields that have practical importance in applications such as MHD generators. From the results of the model, following conclusions can be drawn:

1. In flow of electrically conducting fluid under transverse magnetic fields, the magnetic body force retards the flow.

2. The velocity profiles flatten as Hartmann number increases due to electromagnetic body force.

3. Temperature of the fluid is increased by viscous and ohmic dissipations. However, as Hartmann number increases, viscous dissipation dominates over ohmic dissipation. Thus, as the flow is retarded, temperature of the fluid decreases with decrease in viscous dissipation.

4. In all cases the applied magnetic field affects the flow. However, the effect increases as the wall conductivity

Following can be recommended for future work on MHD flow solutions;

1. In the present applications, the walls of the ducts were either ideally conducting or ideally insulating. However, for a more realistic problem, walls with finite conductivity should be considered.

2. The model can be extended to solve flow over bodies or developing duct flows. In this case a modification should be done to include the nonlinear terms in the governing equations. A simpler solution to this difficult problem can be obtained when the induced field effects are negligible in comparison to applied magnetic field.

3. For applications involving high velocities such as ion accelerators or electrical propulsion e.t.c., compressibility effects should be considered. In this case, Navier - Stokes and energy equations are coupled.

4. A three - dimensional analysis should be carried out for applications such as hypersonic flights. Because of the high speed of the missile or reentry vehicle in the atmosphere, the air may be heated by the boundary layer to a temperature at which the gas is ionized. By applying magnetic field, skin - friction can be affected.

5. The accuracy of the finite element solution can be improved by using a finer mesh structure. However, this will require a larger computer storage.

6. In order to generalize the computer program, an automatic mesh generation scheme [29] should be adopted so that the model can be applied to irregular geometries more easily.

References

1. Karlovitz, B., "Third Symposium on Engineering Aspects of MHD", 1940.
2. Hartmann, J., "Math. - fys. Medd.", 1937.
3. Alfven, H., "Nature", 1942.
4. Grundy, R.F., "MHD Energy for Electric Power Generation", *Noyes Data Corporation*, 1978.
5. Aspnes, J.D., Pierre, D.A., "MHD Power Plant Modelling and Control", *Energy Conversion*, V. 18, 1978.
6. Sodha, M.S., Gupta, B.K., "Power Output of an MHD Generator : Effect of Ionization Instability and Boundary Layer", *Energy Conversion*, V. 19, 1979.
7. Hara, T., "Shape Optimization of the Open Cycle MHD Generator Channel", *7 th International Conference on MHD Electrical Power Generation*, MIT - June 16-20, 1980.
8. Shercliff, J.A., "Steady Motion of Conducting Fluids in Pipes under Transverse Magnetic Fields, *"Proceedings, Cambridge, Phylosophical Society*, V. 49, 1953.
9. Chang, C.C., Lundgren, T.S., "Duct Flow in MHD", *Journal of Applied Mathematics and Physics*, 1961.
10. Ihara, S., Tajima, K., Masushima, A., "The Flow of Conducting Fluids in Circular pipes with Finite Conductivity Under Uniform Transverse Magnetic Fields", *Journal of Applied Mechanics*, V.34, Trans. ASME, V. 89, Series E, 1967.
11. Chu, W.H., "On MHD Flow in Rectangular Duct of Arbitrary Conductivity for Arbitrary Hartmann Number", *Journal of Applied Mechanics*, V. 36, Trans. ASME, V. 91, Series E, Dec. 1969.
12. Tani, I., "Steady Flow of Conducting Fluids in Channels Under Transverse Magnetic Fields with Consideration of Hall Effect", *Journal of Aerospace Sciences*, V. 29, March 1962.
13. Oliver, D.A., Swean, T.F., Markham, D.M., Maxwell, C.D., Demetriades, S.T., "High Magnetic Reynolds number and Strong Interaction Phenomena in MHD Channel Flows" *7 th International Conference on MHD"*, 1980.
14. Trung, D.T., Messerle, H.K., "The Operating Region of MHD Faraday Generators", *7 th Int. Conf. On MHD*, 1980.
15. Miyata, M., "Non-equilibriun Hall MHD Generation. Experiments with Strong J x B Interactions" *7th Int. Conf. on MHD*, 1980.
16. Gherson, H., Lykondis, P.S., Lynch, R.E., "Analytical Study of End Effects in Liquid Metal MHD Generators", *7th Int. Conf. on MHD*, 1980.
17. Asinovskiy, E.I., Lebedef, Y.F., Ostashev, v.y., "Investigation of Processes determining the Efficiency of Energy conversion in a Linear Explosive MHD Generator", *7th. Int. Conf. on MHD.*
18. Sodha, H.S., Gupta, B.K., Maken, N.J.S., "Transpart phenomema in Nonequilibrium MHD Generators", *7th Int. Conf. on MHD*, 1980.
19. Scheindlin, A.E., "Experimental Investigation of the Effect of Boundary Layers on the Characteristic of a MHD Generator." Inst. of High Temperatures, Academy of Sciences of USSR, *Teplofizika Vysokikh Temperatur*, V 11, 1973.
20. Krillov, V.V., Semenov, Y.D., "Investigation of Heat Exchange in an MHD Generator channel", Inst. of High, Temps., *Tepl. Vys. Temperatur*, V11, 1973.
21. Biberman, L.M., Medin, S.A., Mnatsakanian, A.K., "Radiative and Convective Heat Transfer in MHD Generator Duct".
22. Zaporowski, B., Roszkiewicz, J., "Investigation of Heat Transfer from plasma flux to Electrode and Insulating walls of the MHD Generator Channel", *18 th Sym. of Engineering. Aspects of MHD*, Montana, June 18-20, 1979.
23. Sutton, Sherman, *"Engineering Magnetohydrodynamics"*, Mc.Graw—Hill,1966.
24. Shercliff, J.A., *"A Textbook of MHD"*, Mc Graw-Hill, 1964.
25. Finlayson, B.A., *"The Method of Weighted Residuals and Variational Principles"*, Acedemic Press, 1972.
26. Hughes, W.F., *"The Electrodynamics, of Fluids"* John Willy and Sons, Inc., 1966.
27. Norrie, I., *"Introduction to Finite Element Analysis"*, Academic Press, New York, 1974.
28. Zienkiewicz, O.C., *"The Finite Element Method"*, Mc Graw-Hill, London, 1977.
29. Kleinstreuer, C. ; Holdeman .J.T., "A Triangular Finite Element Mesh Generator For Fluid Dynamic Systems of Arbitrary Geometry", *Int. J. for Numerical Methods in Engineering*, V.15. 1980, pp. 1325 - 1334.

APPENDIX A

Review of Magnetohydrodynamics

MHD differs from ordinary hydrodynamics in that the fluid is electrically conducting. It is not magnetic but it affects a magnetic field by electric currents flowing in it. The fluid conducts because it contains free charges (ions or electrons) that can move indefinitely, but it may also be a dielectric and contain bound charges which can only move a limited extent under electric fields. As a consequence of this ability to conduct electricity, the electromagnetic field will give rise to two principal effects: Body forces acting on the fluid will be created and energy will be exchanged with the fluid. Then, for an incompressible fluid, Navier - Stokes and energy equations are;

$$\rho \frac{D\underset{\sim}{v}}{Dt} = -\nabla p + \mu \nabla^2 \underset{\sim}{v} + \underset{\sim}{F} \tag{A.1}$$

$$\rho \frac{D}{Dt} \left(\frac{1}{2} \underset{\sim}{v}.\underset{\sim}{v} + e\right) = - \underset{\sim}{\nabla}\cdot\underset{\sim}{q} + Qem + visc. \tag{A.2}$$

where,

$\underset{\sim}{F}$; gravitational and electromagnetic body force field.

Qem; rate at which electromagnetic field is doing work on the charges.

In deriving the additional terms in equations (A.1) and (A.2), the electromagnetic theory is to be reviewed. Since the velocities are much smaller than the speed of light, nonrelativistic theory will be discussed.

A charged particle is mainly subjected to three kinds of forces;

1. It is repelled or attracted by other charged particles, the total force on the particle per unit of its charge due to all the other charges present being the electrostatic field E_s From Coulomb's law,

$$\text{curl } \underset{\sim}{E}_s = 0 \tag{A.3}$$

therefore, it can be expressed as the gradient of an electrostatic potential,

$$\underset{\sim}{E}_s = -\underset{\sim}{\nabla}\phi \tag{A.4}$$

It follows that in regions where there is a net charge q per unit volume [24];

$$\text{div } \underset{\sim}{E}_s = q/Ko \tag{A.5}$$

where, Ko is the permittivity of vacuum.

2. Charged particles in motion produce the phenomenon of magnetism which is described by the magnetic field $\underset{\sim}{B}$.If a particle is moving with a velocity u, that it will be exposed to a magnetic force, $\underset{\sim}{F}_B$ per unit of its charge;

$$\underset{\sim}{F}_B = \underset{\sim}{u} \times \underset{\sim}{B} \tag{A.6}$$

3. If the magnetic field is changing with time, then per unit of its charge, a particle will be subjected to an additional force $\underset{\sim}{E}i$, the induced electric field, defined by;

$$\operatorname{div} \underset{\sim}{E}_I = 0 \qquad (A.7)$$

and by Faraday's law;

$$\operatorname{curl} \underset{\sim}{E}_I = -\frac{\partial \underset{\sim}{B}}{\partial t} \qquad (A.8)$$

The latter implies that

$$\frac{\partial}{\partial t}(\operatorname{div} \underset{\sim}{B}) = 0$$

or

$$\operatorname{div} \underset{\sim}{B} = C \qquad (A.9)$$

Actually there is a stronger condition on $\underset{\sim}{B}$ [23] ;

$$\operatorname{div} \underset{\sim}{B} = 0 \qquad (A.10)$$

The combined electric field $\underset{\sim}{E}$, is then given as;

$$\underset{\sim}{E} = \underset{\sim}{E}_s + \underset{\sim}{E}_I \qquad (A.11)$$

It follows that,

$$\operatorname{curl} \underset{\sim}{E} = -\frac{\partial \underset{\sim}{B}}{\partial t} \qquad (A.12)$$

$$\operatorname{div} \underset{\sim}{E} = q/Ko \qquad (A.13)$$

The total force field is obtained by superposing electric and magnetic fields ;

$$\underset{\sim}{f} = \underset{\sim}{E} + \underset{\sim}{u} \times \underset{\sim}{B} \qquad (A. 14)$$

This is called the Lorentz force.

To describe the situation where there is a spatial distribution of moving charges we need another vector $\underset{\sim}{J}$, the current density, which includes the net flow of all charges. For nonmagnetic materials the magnetic field, current density and electric field are related by Ampere - Maxwell law;

$$\operatorname{curl} \underset{\sim}{B}/\mu_o = \underset{\sim}{J} + Ko\,\frac{\partial \underset{\sim}{E}}{\partial t} \qquad (A.15)$$

where μ_o is the permeability of vacuum.

The last term in Eq (A.15) is Maxwell's contribution.

Consider a conducting material containing positive and negative charged particles. Let a particle of charge p have a velocity $\underset{\sim}{u}$. Then net charge (free and bound) per unit volume is given by

$$\Sigma p = q \tag{A.16}$$

and the net current density is given by

$$\Sigma p\underset{\sim}{u} = \underset{\sim}{J} \tag{A.17}$$

Since the Lorentz force on a particle is $p(\underset{\sim}{E} + \underset{\sim}{u} x \underset{\sim}{B})$, the total force per unit volume is given by

$$\underset{\sim}{F}em = q\underset{\sim}{E} + \underset{\sim}{J} x \underset{\sim}{B} \tag{A.18}$$

In a stationary conductor, free charges drifting under the action of Lorentz force are also subjected to a drag force due to collisions equal to $k\underset{\sim}{u}$, where k is some constant for each particle. Neglecting inertia, force balance on each particle leads to

$$p(\underset{\sim}{E} + \underset{\sim}{u} \times \underset{\sim}{B}) = k\underset{\sim}{u} \tag{A.19}$$

Summing over the free charges in the element of conductor one writes;

$$q\ \underset{\sim}{E} + \underset{\sim}{J}_c x \underset{\sim}{B} = \Sigma k\underset{\sim}{u}$$

or

$$\underset{\sim}{E} + \underset{\sim}{J}_c x \underset{\sim}{B}/q \quad = \Sigma\, k\underset{\sim}{u}/q \tag{A.20}$$

where,

$\underset{\sim}{J}c$: conduction current due to drift of free charges

q ; net free charge per unit volume.

The righthand side of Eq (A.20) has been shown to be proportional to $\underset{\sim}{J}$ [24],

$$\underset{\sim}{E} + \underset{\sim}{J}_c \times \underset{\sim}{B}/q \ = \underset{\sim}{J}_c/\sigma \tag{A.21}$$

where, σ is the electrical conductivity of the material.

The term in Eq. (A.21) due to B is refered to as the Hall effect. If the free charges are electrons with charge $-e$ and number density n;

$$\underset{\sim}{E} - \underset{\sim}{J} x \underset{\sim}{B}/ne = \underset{\sim}{J}/\sigma \tag{A.22}$$

The Hall effect is due to the transverse magnetic force on the drifting free charges, which is negligible for low magnetic fields [26].

when the conductor is moving at a velocity $\underset{\sim}{v}$, the velocity of a particle is $\underset{\sim}{v}+\underset{\sim}{u}$. Summing over all charges,

$$\underset{\sim}{J} = \Sigma p\,(\underset{\sim}{v}+\underset{\sim}{u})$$

$$= \underset{\sim}{J}_v + \underset{\sim}{J}_c + \underset{\sim}{J}_p$$

where, $\underset{\sim}{J}_v$; convection current: $q\,\underset{\sim}{v}$
$\underset{\sim}{J}_c$: conduction current due to free charges
$\underset{\sim}{J}_p$: polarization current due to bound charges $\dfrac{\partial \underset{\sim}{P}}{\partial t}$

and $\underset{\sim}{P}$ is dipole moment [23].

Then the balance of forces on a free charge leads to Ohm's law;

$$\underset{\sim}{J}_c = \sigma(\underset{\sim}{E} + \underset{\sim}{v} \times \underset{\sim}{B}) \tag{A.23}$$

and due to motion of bound charges

$$\underset{\sim}{J} = q\underset{\sim}{v} + \sigma\,(\underset{\sim}{E} + \underset{\sim}{v} \times \underset{\sim}{B}) + \frac{\partial \underset{\sim}{P}}{\partial t} \tag{A.24}$$

MHD Approximations

Order of magnitude analysis for low - frequency electromagnetism and MHD leads to;

i. The ratio, curl $\underset{\sim}{B}/\mu_o$:Ko $\partial E/\partial t$ in Eq (A.15) is of order $B/\mu_o\,d$:KoEf (if B and E are typical magnitudes and d and f are length scale and frequency), then using Eq (A.8);

$$\frac{\text{Curl } \underset{\sim}{B}/\mu_o}{K_o\ \partial \underset{\sim}{E}/\partial t} \sim \frac{B/\mu_o\ d}{K_o\ Ef} \sim \frac{1}{K_o \mu_o d^2 f^2} \sim \frac{\lambda^2}{d^2}$$

where,

$$\lambda = c/f, \quad c^2 = 1/K_o\mu_o$$

This ratio is very large and the Maxwell term ($K_o\ \partial \underset{\sim}{E}/\partial t$) in Eq (A.15) is negligible unless the frequency is very high.

Therefore Eq (A.15) reduces to:

$$\text{curl } \underset{\sim}{B}/\mu_o = \underset{\sim}{J} \tag{A.25}$$

and furthermore,

$$\text{div } \underset{\sim}{J} = 0 \tag{A.26}$$

Eqs (A.25) and (A.26) are Ampere's law and Kirchhoff's first law respectively.

ii. It is noted in Eq (A.13) that total charge density q is of order,

$$q \sim K_o E/d \sim K_o Bv/d,$$

thus the convection current is of order

$$q\underset{\sim}{v} \sim K_o Bv^2/d$$

while from Eq (A.25), the total current is of order

$$\underset{\sim}{J} \sim B/\mu_o d$$

consequently,

$$q\underset{\sim}{v}/\underset{\sim}{J} \sim v^2/c^2 \ll 1$$

and thus it can be neglected.

Furthermore, the polarization current is also of the order of $K_o \partial\underset{\sim}{E}/\partial t$ [23], therefore, the conduction current in Eq. (A.23) can be replaced by the total current:

$$\underset{\sim}{J} = \sigma(\underset{\sim}{E} + \underset{\sim}{v} \times \underset{\sim}{B}) \tag{A.27}$$

iii. The relative order of magnitudes of the electric and magnetic components of the body force in Eq (A.18) are as follows:

$$\frac{q\underset{\sim}{E}}{\underset{\sim}{J}\times\underset{\sim}{B}} \sim \frac{K_o E^2/d}{B^2/\mu_o d} \sim \frac{K_o B^2 v^2/d}{B^2/\mu_o d} \sim \frac{v^2}{c^2} \ll 1$$

therefore, $q\underset{\sim}{E}$ in Eq. (A.18) can be neglected.

With these simplifications, the resulting equations are;

$$\text{curl}\, \underset{\sim}{B}/\mu_o = \underset{\sim}{J} \quad \text{(Ampere's law)}$$

$$\underset{\sim}{J} = \sigma(\underset{\sim}{E} + \underset{\sim}{v} \times \underset{\sim}{B}) \quad \text{(Ohm's law)}$$

and the body force on the charged particles;

$$\underset{\sim}{F}em = \underset{\sim}{J} \times \underset{\sim}{B} \tag{A.28}$$

Hence, Navier - Stokes equations in the absence of gravitational forces becomes;

$$\rho \frac{D\underset{\sim}{v}}{Dt} = -\underset{\sim}{\nabla} p + \mu\nabla^2 \underset{\sim}{v} + \underset{\sim}{J}\times\underset{\sim}{B} \tag{A.29}$$

Since charges within a material move under the action of electromagnetic forces, colliding and exchanging energy with the rest of the material, electrical work can be done on or by the material. A single particle of charge p, moving with a velocity u, experiences the Lorentz force, $p(\underset{\sim}{E}+\underset{\sim}{u}\times\underset{\sim}{B})$, which does work on it at a rate:

$$\frac{dW}{dt} = p(\underset{\sim}{u}.\underset{\sim}{E}) + p\underset{\sim}{u}.(\underset{\sim}{u}\times\underset{\sim}{B}) \tag{A.30}$$

The second term vanishes because the force is perpendicular to the motion. Then, summing over such charges in an element, the electromagnetic field does work on the charges at a rate

$$
\begin{aligned}
Qem &= (\Sigma p\underset{\sim}{u}).\underset{\sim}{E} \\
&= \underset{\sim}{J}.\underset{\sim}{E}
\end{aligned}
\tag{A.31}
$$

per unit volume of the element. From Ohm's Law, Eq (A.27)

$$\underset{\sim}{E} = \underset{\sim}{J}/\sigma - \underset{\sim}{v} \times \underset{\sim}{B} \tag{A.32}$$

Hence,

$$
\begin{aligned}
Qem &= \underset{\sim}{J}.\underset{\sim}{J}/\sigma - \underset{\sim}{J}.(\underset{\sim}{v}\times\underset{\sim}{B}) \\
&= \underset{\sim}{J}.\underset{\sim}{J}/\sigma + \underset{\sim}{v}.(\underset{\sim}{J}\times\underset{\sim}{B})
\end{aligned}
\tag{A.33}
$$

The first term is the Ohmic dissipation and the second term is the rate at which electromagnetic force does work.

Substituting Eq (A.33) into Eq (A.2), overall energy equation becomes:

$$\rho \frac{D}{Dt}\left(\frac{1}{2}\underset{\sim}{v}.\underset{\sim}{v} + e\right) = -\underset{\sim}{\nabla}\underset{\sim}{q} + \underset{\sim}{J}.\underset{\sim}{J}/\sigma + \underset{\sim}{v}.\underset{\sim}{J}\times\underset{\sim}{B} + \text{visc.} \tag{A.34}$$

Multiplying Eq (A.29) with $\underset{\sim}{v}$, the mechanical equation is obtained:

$$\underset{\sim}{v}.\left(\rho \frac{D\underset{\sim}{v}}{Dt} + \underset{\sim}{\nabla} p\right) = \underset{\sim}{v}.(\underset{\sim}{J}\times\underset{\sim}{B}) + \quad v.\nabla^2 v \tag{A.35}$$

Subtracting Eq (A.35) from Eq (A.34), thermal energy equation is obtained:

$$\rho \frac{De}{Dt} = \phi - \underset{\sim}{\nabla}.\underset{\sim}{q} + \underset{\sim}{J}.\underset{\sim}{J}/\sigma \tag{A.36}$$

where ϕ is the viscous dissipation.

Using perfect gas relation and Fourier heat conduction law,

$$\frac{De}{Dt} = c_v \frac{DT}{Dt} \tag{A.37}$$

$$\underset{\sim}{q} = -\kappa \underset{\sim}{\nabla} T \tag{A.38}$$

and defining magnetic field strength

$$\underset{\sim}{H} = \underset{\sim}{B}/\mu_o \tag{A.39}$$

and from Eq (A.25)

$$\underset{\sim}{J} = \text{curl } \underset{\sim}{B}/\mu_o = \text{curl } \underset{\sim}{H}$$

one obtaines,

$$c_v \frac{DT}{Dt} = \kappa \nabla^2 T + \Phi + (\nabla \times \underset{\sim}{H}) . (\nabla \times \underset{\sim}{H}) / \sigma \tag{A.40}$$

Hence governing equations for MHD are derived which are summarized below;

Navier - Stokes equations;

$$\rho \frac{D\underset{\sim}{v}}{Dt} = -\underset{\sim}{\nabla} p + \mu \nabla^2 \underset{\sim}{v} + \mu_o \underset{\sim}{J} x \underset{\sim}{H} \tag{A.41}$$

Energy equation;

$$\rho c_v \frac{DT}{Dt} = \kappa \nabla^2 T + \Phi + \underset{\sim}{\nabla} \times \underset{\sim}{H} . \underset{\sim}{\nabla} \times \underset{\sim}{H} / \sigma \tag{A.42}$$

Ohm's law:

$$\underset{\sim}{J} = \sigma (\underset{\sim}{E} + \underset{\sim}{v} \times \underset{\sim}{B}) \tag{A.43}$$

with the Maxwells relations;

$$\begin{aligned} &\text{curl } \underset{\sim}{H} = \underset{\sim}{J} \\ &\text{div } \underset{\sim}{H} = 0 \\ &\text{curl } \underset{\sim}{E} = - \quad \partial \underset{\sim}{B} / \partial t \\ &\text{div } \underset{\sim}{E} = q / Ko \end{aligned} \tag{A. 44}$$

The last equation is not necessary for solving MHD - flow problems since charge distribution is of no interest. However, in some applications the effect of q should be included [24]. In the present study, it will be ommitted.

APPENDIX B

Finite Element Methods

In the finite element methods the continuous problem is divided into finite number of elements such that the dependent variables are approximated over each element and hence over the whole domain. Thus the continuous problem is transformed into a discrete problem, solution of which yields an approximate solution for the domain [27,28].

The elements that discretize the domain are classified most generally into one, two and three - dimensional categories. In all these categories, a general trial function can be represented over an element as;

$$u = \underset{\sim}{N}\underset{\sim}{u} \tag{B.1}$$

where N is the shape function matrix and u is the element nodal vector.

For a Lagrangian element there is only one degree of freedom, i.e. one unkrown per node , and hence Eq (B.1) can be written as;

$$u = [N_1 N_2 .... N_s] \begin{bmatrix} u_1 \\ u_2 \\ \\ \\ u_s \end{bmatrix} \tag{B.2}$$

where 1,2, ...s are node identifiers and s is the total number of nodes

1. One - dimensional elements
   Let the solution domain discretized by linear elements,

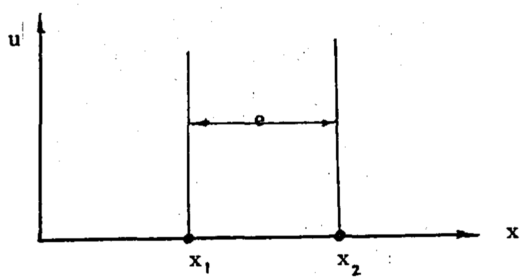

Fig. 30 One - dimensional element

the trial function u will have the form over each element

$$u = c_1 + c_2 x \tag{B.3}$$

where c and c are constants. Evaluating Eq (B.3) on each node of an element;

$$u_1 = c_1 + c_2 x_1$$
$$u_2 = c_1 + c_2 x_2$$

solving for c_1 and c_2

$$c = \frac{x_2 u_1 x_1}{x_2 - x_1}; \qquad c = \frac{u_2 - u_1}{x_2 - x_1} \tag{B.4}$$

Substitute Eq. (B.4) into Eq. (B.3) and rearrange,

$$u = \frac{x_2 - x}{x_2 - x_1} u_1 + \frac{x - x_1}{x_2 - x_1} u_2 \tag{B.5}$$

Eq. (B.5) is of the form

$$u = N_1 u_1 + N_2 u_2 \tag{B.6}$$

where,

$$N_1 = \frac{x_2 - x}{x_2 - x_1} \; ; \quad N_2 = \frac{x - x_1}{x_2 - x_1} \tag{B.7}$$

choosing a coordinate system peculiar to an element such that $L_1 = 1$ at $x = x_1$ and $L_1 = 0$ at $x = x_2$, namely natural coordinates,

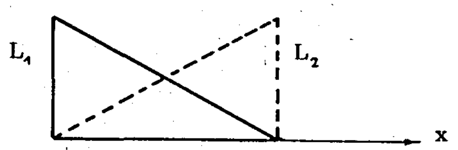

Fig. 31. Natural coordinates in one-dimension

Hence, the approximation u across the element e can be interpolated as,

$$u = L_1(x)\, u_1 + L_2(x)\, u_2 \tag{B.8}$$

Comparing Eq. (B.8) with Eq. (B.6) shows that the shape functions N_1 and N_2 are given by

$$N_1 = L_1(x) \; ; \quad N_2 = L_2(x) \tag{B.9}$$

The following relation is valid for natural coordinates [28];

$$\int L_1^a \; L_2^b \; dx = \frac{a!\, b!}{(a+b+1)!} (x_2 - x_1) \tag{B.10}$$

2. Two - dimensional elements

Consider a typical triangular element with nodes j, j, m,

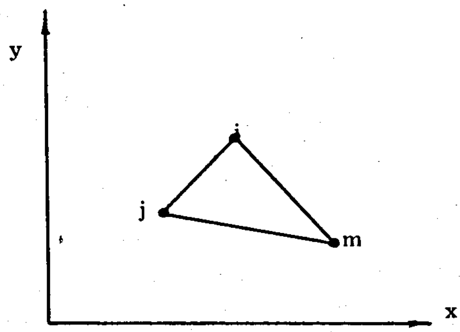

Fig. 32. A triangular element.

The trial function for the element will be;

$$u = c_1 + c_2 x + c_3 y \tag{B.11}$$

evaluating at each node of an element,

$$\begin{aligned} u_i &= c_1 + c_2 x_i + c_3 y_i \\ u_j &= c_1 + c_2 x_j + c_3 y_j \\ u_m &= c_1 + c_2 x_m + c_3 y_m \end{aligned} \tag{B.12}$$

The system of equations (B.12) will have a unique solution for c provided the determinant of the coefficient matrix does not vanish, i.e. ;

$$2\Delta = \begin{vmatrix} 1 & x_i & y_i \\ 1 & x_j & y_j \\ 1 & x_m & y_m \end{vmatrix} \neq 0 \tag{B.13}$$

Solving for c 's from Eqs (B.12)

$$\begin{aligned} c_1 &= \frac{1}{2\Delta}(a_i u_i + a_j u_j + a_m u_m) \\ c_2 &= \frac{1}{2\Delta}(b_i u_i + b_j u_j + b_m u_m) \\ c_3 &= \frac{1}{2\Delta}(c_i u_i + c_j u_j + c_m u_m) \end{aligned} \tag{B.14}$$

where,

$$a_i = x_j y_m - x_m y_j \; ; \; b_i = y_j - y_m , \; c_i = x_m - x_j$$

others are obtained by cyclic permutation of the indices.

Substitution of Eqs (B.14) into Eq (B.11) results with the trial function:

$$u = \frac{1}{2\Delta}[(a_i + b_i x + c_i y) u_i + (a_j + b_j x + c_j y) u_j + (a_m + b_m x + c_m y) u_m] \quad (B.15)$$

Comparing Eq (B.15) with Eq (B.1)

$$\begin{aligned} N_i &= \frac{1}{2\Delta}(a_i + b_i x + c_i y) \\ N_j &= \frac{1}{2\Delta}(a_j + b_j x + c_j y) \\ N_m &= \frac{1}{2\Delta}(a_m + b_m x + c_m y) \end{aligned} \quad (B.16)$$

Introduce natural coordinates in two - dimensions, which are referred to as area coordinates,

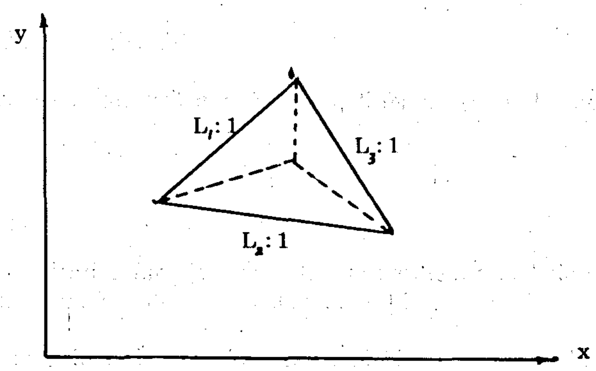

Fig. 33. Area coordinates

the approximation u across an element becomes,

$$u = L_1 u_1 + L_2 u_2 + L_3 u_3 \quad (B.17)$$

therefore, for the triangular element

$$N_1 = L_1;\ N_2 = L_2;\ N_3 = L_3 \quad (B.18)$$

It can be shown that the relation between cartesian and natural coordinates is given by [28] ;

$$\begin{bmatrix} x \\ y \\ 1 \end{bmatrix} = \begin{bmatrix} x_1 & x_2 & x_3 \\ y_1 & y_2 & y_3 \\ 1 & 1 & 1 \end{bmatrix} \begin{bmatrix} L_1 \\ L_2 \\ L_3 \end{bmatrix} \quad (B.19)$$

Similar to Eq (B.10), the following relation holds for area coordinates:

$$\int L_1^a\ L_2^b\ L_3^c\ dD = \frac{a!\ b!\ c!}{(a+b+c+2)!} 2\Delta \quad (B.20)$$

3. Residual Finite Element Methods

Consider a governing differential equation in the domain D which involves one dependent variable u and several independent variables x_j,

$$\mathcal{L}(u;x_j) = 0 \tag{B.21}$$

Substitution of an approximate solution u will result an error, or residual $\bar{R}$:

$$R = \mathcal{L}(u;x_j) - \mathcal{L}(u;x_j) \tag{B.22}$$

by Eq (B.21),

$$R = -\mathcal{L}(u;x_j) \tag{B.23}$$

In residual methods, the residual R in Eq (B.23) is required to be small, or the weighted integral over the domain is required to

$$\int w\,\mathcal{L}(u;x_j)\,dD = 0 \tag{B.24}$$

where w is the weighting function.

Depending on the choice of the weighting function, different approaches can be rediscovered [27].

Galerkin Residual Methods

In this method, the weighting functions are taken to be the interpolation functions which leads in general to the best approximation among other Residual methods [25].

Galerkin method forces the residual to be zero by making it orthogonal to each member of a complete set of functions, i.e;

$$\int N_i\,\mathcal{L}(u;x_j)\,dD = 0 \tag{B.25}$$

APPENDIX C

Derivation of the element equations.

Finite element discretization of the governing differential equations, leads to a set of algebraic equations Hence, for a particular element,

$$[k]\,(u) = (f) \tag{C.1}$$

In the above equation, the stiffness matrix k and right hand-side f would contain domain integrals which could be easily evaluated by certain analytic expressions.

In the one-dimensional formulation, the element equations are of the form Eq (C.1), where,

$$k = \int \left(\frac{dN_i}{dn}\,\frac{dN_j}{dn} + Ha^2\, N_i N_j\right) dn\ . \tag{C.2}$$

$$f = C \int N_i\, dn \tag{C.3}$$

Using linear interpolation functions, Eqs (C.2) and (C.3) become:

$$k \;=\; \int \left(\frac{dL_i}{dn}\,\frac{dL_j}{dn} + Ha^2\, L_i L_j\right) dn \tag{C.4}$$

$$f = C \int L_i\, dn \tag{C.5}$$

Performing the integrals in Eqs. (C.4) and (C.5) by using Eq (B.10),

$$k = \frac{1}{h}\begin{bmatrix} 1 + Ha^2 h^2/3 & -1 + Ha^2h^2/6 \\ -1 + Ha^2h^2/6 & 1+Ha^2h^2/3 \end{bmatrix} \tag{C.6}$$

$$f = C\,\frac{h}{2}\begin{bmatrix}1\\1\end{bmatrix} \tag{C.7}$$

where, h is the length of the element.

For the two-dimensional formulation, a similar procedure can be carried out. Eqs (2.22) can be combined in a single matrix equation for an element;

$$[k]\,(\psi) = (r) \tag{C.8}$$

where,

$$k = \begin{bmatrix} k_1 & k_2 \\ k_2 & k_1 \end{bmatrix}, \quad \psi = \begin{bmatrix} H \\ u \end{bmatrix}, \quad r = \begin{bmatrix} 0 \\ f \end{bmatrix} \tag{C.9}$$

and,

$$k_1 = \iint \left(\frac{\partial N_i}{\partial y} \frac{\partial N_j}{\partial y} + \frac{\partial N_i}{\partial z} \frac{\partial N_j}{\partial z} \right) dydz$$

$$k_2 = - \frac{Ha}{k} \iint \frac{\partial N_j}{\partial y} N_i dy\, dz \tag{C.10}$$

$$f = \iint N\, dy\, dz$$

Using linear interpolation functions and by Eq (B.20);

$$k_1 = (c_i\, c_j + b_i\, b_j) / 4\Delta$$

$$k_2 = Ha\, c_j / 6k \qquad i = 1,2,3 \tag{C.11}$$

$$f = -\Delta/3 \qquad i = 1,2,3$$

For the temperature field , we have a similar equation;

$$[k_1](T) = (r)_T \tag{C.12}$$

where,

$$r_T = \iint N_i [H\nabla N_j \nabla N_j H + u\nabla N_j \nabla N_j u] dy\, dz$$

$$= (c_l\, c_m + b_l\, b_m)(H_l\, H_m + u_l\, u_m) / 12\Delta \tag{C.13}$$

In the above, summation convention has been used.

APPENDIX D

Computer Program

The flowchart of the computer program to solve the system of differential equations (Eqs 2.7, 2.8 and 2.15) is given with description of the subroutines in the following:

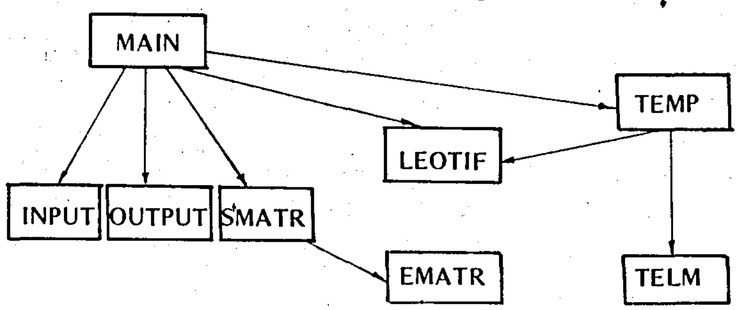

Fig. 34. Computer program flowchart

INPUT: Reads input data and initializes the program.

SMATR : Calculates necessary coefficients to evaluate element matrices, assembles element matrices calculated through subroutine EMATR and finally inserts natural boundary conditions.

EMATR : Calculates element matrices.

TEMP : Subprogram to calculate the temperature field.

TELM : Forms element matrices of the energy equation.

OUTPUT : Prints out the results.

LEOTIF : Solves system of linear algebraic equations.

The listing of the computer program is given in the following.

```
      PARAMETER N=6,M=3,NN=242,NPOIN=121,NELEM=200
      COMMON/INP/NOD(NELEM,N),X(NPOIN),Y(NPOIN),NPT(NN),NMP(NN),VAL(NN)
      COMMON/ELEMT/STE(NELEM,N,N),SM(NN,NN),RR(NELEM,N),R(NN)
      COMMON/SYST/A(M),B(M),C(M),DELTA
      COMMON/SYST2/BB(NELEM,M),CC(NELEM,M),DEL(NELEM),AA(NELEM,M)
      COMMON/INP2/IPLOT,IPRINT,LIN,NEUMN,NPRES,T,H(10),NH,HA,KCALL
      COMMON/EL2/HX(M),U(M)
      COMMON ITEMP
      DIMENSION WKAREA(NN)
C     ***************************************
C     PROGRAM TO SOLVE MHD FLOW PROBLEMS BY
C     FINITE ELEMENT METHODS
C     ***************************************
C
C     INITIALIZE PROGRAM
C
      CALL INPUT
      DO 80 I=1,NH
      KCALL=0
      HA=H(I)
C
C     GENERATE STIFFNESS MATRIX
C
      CALL SMATR
      IF (LIN-1) 60,50,50
   50 CONTINUE
C
C     SOLVE SYSTEM OF EQUATIONS
C
      CALL LEQT1F (SM,1,NN,NN,R,0,WKAREA,IER)
      GO TO 70
   60 CALL ITERN
   70 CONTINUE
      CALL OUTPUT
      IF (ITEMP.EQ.0) GO TO 80
      KCALL=1
      CALL TEMP
   80 CONTINUE
      STOP
      END
```

```
      SUBROUTINE INPUT
      PARAMETER N=6,M=3,NN=242,NPOIN=121,NELEM=200
      COMMON/INP/NOD(NELEM,N),X(NPOIN),Y(NPOIN),NPT(NN),NMP(NN),VAL(NN)
      COMMON/INP2/IPLOT,IPRINT,LIN,NEUMN,NPRES,T,H(10),NH,HA,KCALL
      COMMON ITEMP
      INTEGER HEADG(80)
C
C     READS AND PRINTS INPUT DATA
C
C     HEADG=HEADING OF THE PROGRAM
C     NDIM=DIMENSION OF THE PROBLEM
C     LIN=1 IF PROBLEM IS LINEAR
C         0 IF NONLINEAR
C     ITEMP=1 IF TEMPERATURE FIELD IS TO BE SOLVED
C     IPLOT=1 PLOTS THE RESULTS
C     IPRINT=1 ELEMENT STIFFNESS MATRICES ARE PRINTED
C     NEUMN=NODES WHERE FLUX IS SPECIFIED
C     NPRES=NUMBER OF PRESCRIBED NODES
C     T=HEIGHT TO WIDTH RATIO OF THE DUCT
C     H=HARTMANN NUMBER
C
      READ(5,160) (HEADG(I),I=1,80)
      READ(5,10) NDIM,LIN,ITEMP,IPLOT,IPRINT,NEUMN,NPRES
      READ(5,15) NH,T,(H(I),I=1,NH)
      READ(5,20) (K,(NOD(I,J),J=1,M),I=1,NELEM)
      READ(5,30) (Y(I),X(I),I=1,NPOIN)
      READ(5,40) (NPT(I),VAL(I),I=1,NPRES)
      READ(5,170) (NMP(I),I=1,NEUMN)
C
C     PRINT OUT DATA
C
      WRITE(6,180)
      WRITE(6,160) (HEADG(I),I=1,80)
      WRITE(6,50) NPOIN
      WRITE(6,60) NELEM
      WRITE(6,25) NDIM,LIN,ITEMP,IPLOT,IPRINT,NEUMN,NPRES
      WRITE(6,70)
      WRITE(6,80)
      WRITE(6,90) (I,X(I),Y(I),I=1,NPOIN)
      WRITE(6,100)
      WRITE(6,110)
      WRITE(6,120) (I,(NOD(I,J),J=1,M),I=1,NELEM)
      WRITE(6,130)
      WRITE(6,140)
      WRITE(6,150) (NPT(I),VAL(I),I=1,NPRES)
   10 FORMAT(7I5)
   15 FORMAT(I3,F7.3,10F5.2)
   20 FORMAT(24I3)
   25 FORMAT(//,5X,7I5)
   30 FORMAT(22F3.1)
   40 FORMAT(7(I3,F7.2))
   50 FORMAT(////,1X,,NUMBER OF NODES,,I5)
   60 FORMAT(1X,,NUMBER OF ELEMENTS,I5)
   70 FORMAT(///,1X,,X AND Y COORDINATES,,/)
   80 FORMAT(1X,17H NODE      X        Y,2(21H      NODE     X        Y))
```

```
 90 FORMAT((1X,I3,F8.2,F7.2,2(I6,F8.2,F7.2)))
100 FORMAT(1H1,////,1X,,THE ELEMENTS AND THEIR NODES,,/)
110 FORMAT(1X,13HELEM  I  J  M,3(16H   ELEM  I  J  M))
120 FORMAT(1X,I3,I4,2I3,I6,I4,2I3,I6,I4,2I3,I6,I4,2I3)
130 FORMAT(1H1,//////,1X,,NODES WITH PRESCRIBED VALUES,)
140 FORMAT(1X,12H NODE  VALUE,3(15H    NODE  VALUE))
150 FORMAT((1X,I3,F9.3,3(I6,F9.3)))
160 FORMAT(80A1)
170 FORMAT(16I5)
180 FORMAT(1H1,////,1X,,FOLLOWING IS THE INPUT TO FEM PROGRAM FOR ,,/)
    RETURN
    END
```

```
    SUBROUTINE SMATR
    PARAMETER N=6,M=3,NN=242,NPOIN=121,NELEM=200
    COMMON/INP/NOD(NELEM,N),X(NPOIN),Y(NPOIN),NPT(NN),NMP(NN),VAL(NN)
    COMMON/ELEMT/STE(NELEM,N,N),SM(NN,NN),RR(NELEM,N),R(NN)
    COMMON/SYST/A(M),B(M),C(M),DELTA
    COMMON/INP2/IPLOT,IPRINT,LIN,NEUMN,NPRES,T,H(10),NH,HA,KCALL
    COMMON/EL2/HX(M),U(M)
    COMMON/SYST2/BB(NELEM,M),CC(NELEM,M),DEL(NELEM),AA(NELEM,M)
    DIMENSION NSUR(NPOIN,NPOIN),XX(M),YY(M)
    DIMENSION NT(NN)
                  Λ
    CALCULATES SYSTEM STIFFNESS

    DO 10 I=1,NPOIN
 10 NSUR(I,1)=0
    DO 30 I=1,NELEM
    DO 20 J=1,M
    LK=NOD(I,J)
    NSUR(LK,1)=NSUR(LK,1)+1
    LL=NSUR(LK,1)+1
 20 NSUR(LK,LL)=I
 30 CONTINUE
    DO 90 I=1,NELEM
    DO 40 J=1,M
    NOD(I,J+M)=NOD(I,J)
    LK=NOD(I,J)
    HX(J)=R(LK)
    U(J)=R(LK+NPOIN)
    XX(J)=X(LK)
 40 YY(J)=Y(LK)

    CALCULATE A,B,C

    DO 80 J=1,M
    LK=J+1
    LL=J+2
    IF (LK-M) 70,60,50
 50 LK=1
```

```
      LL=2
   60 LL=1
   70 A(J)=XX(LK)*YY(LL)-XX(LL)*YY(LK)
      B(J)=YY(LK)-YY(LL)
   80 C(J)=XX(LL)-XX(LK)
      DELTA=(C(3)*B(2)-C(2)*B(3))/2.
      IF (KCALL.EQ.1) GO TO 81
C
C     CALCULATE ELEMENT STIFFNESS MATRICES
C
      CALL EMATR(I)
      GO TO 82
   81 CALL TELM(I)
      GO TO 90
   82 CONTINUE
      DO 86 K=1,NEUMN
      IF (I.NE.NMP(K)) GO TO 86
      ICALL=1
      DO 85 J=1,M
      AA(I,J)=A(J)
      BB(I,J)=B(J)
   85 CC(I,J)=C(J)
      DEL(I)=DELTA
   86 CONTINUE
   90 CONTINUE
      DO 110 I=1,NN
      DO 100 J=1,NN
  100 SM(I,J)=0.
  110 R(I)=0.
      IF (KCALL.EQ.1) ICALL=0
      IF (ICALL.EQ.1) CALL NBCS
      DO 230 NODE=1,NN
      IF (NODE-NPOIN) 130,130,140
  130 ND=NODE
      GO TO 150
  140 ND=NODE-NPOIN
C
C     INSERT BOUNDARY CONDITIONS
C
  150 CONTINUE
      DO 155 I=1,NPRES
      IF (KCALL.EQ.1) GO TO 154
      IF (NODE-NPT(I)) 155,160,155
  154 NT(I)=NPT(I)-NPOIN
      IF (NODE.EQ.NT(I)) GO TO 160
  155 CONTINUE
      GO TO 170
  160 SM(NODE,NODE)=1.
      R(NODE)=VAL(I)
      GO TO 230
  170 CONTINUE
      IE=NSUR(ND,1)
      IEL=IE+1
      DO 220 ITEL=2,IEL
      LEL=NSUR(ND,ITEL)
```

```
      DO 180 I=1,M
      IR=I
      IF (NODE.GT.NPOIN) IR=IR+M
      IF (NOD(LEL,I)-ND)180,200,180
  180 CONTINUE
      WRITE(6,190)
  190 FORMAT(//,5X,'ERROR IN NUMBERING',//)
      GO TO 240
C
C     ASSEMBLE ELEMENT MATRICES TO FORM SYSTEM MATRIX   A
C
  200 CONTINUE
      DO 210 IC=1,N
      ICO=NOD(LEL,IC)
      IF (IC.GT.M) ICO=ICO+NPOIN
  210 SM(NODE,ICO)=SM(NODE,ICO)+STE(LEL,IR,IC)
      R(NODE)=R(NODE)+RR(LEL,IR)
  220 CONTINUE
  230 CONTINUE
  240 RETURN
      END



      SUBROUTINE EMATR(I)
      PARAMETER N=6,M=3,NN=242,NPOIN=121,NELEM=200
      COMMON/ELEMT/STE(NELEM,N,N),SM(NN,NN),RR(NELEM,N),R(NN)
      COMMON/INP2/IPLOT,IPRINT,LIN,NEUMN,NPRES,T,H(10),NH,HA,KCALL
      COMMON/EL2/HX(M),U(M)
      COMMON/SYST/A(M),B(M),C(M),DELTA
C
C     CALCULATES ELEMENT STIFFNESS MATRICES
C
      DO 10 J=1,3
      RR(I,J)=0.
      DO 10 K=1,3
      STE(I,J,K)=(C(J)*C(K)+B(J)*B(K))/(4.0*DELTA)
   10 STE(I,J+3,K+3)=STE(I,J,K)
      DO 20 J=1,3
      DO 20 K=4,6
      STE(I,J,K)=-(HA/(6.*T))*C(K-3)
   20 STE(I,J+3,K-3)=STE(I,J,K)
      DO 30 J=1,3
   30 RR(I,J+3)=DELTA/3.
      IF (IPRINT.EQ.0) GO TO 50
      WRITE(6,40) I,((STE(I,J,K),K=1,6),J=1,6)
   40 FORMAT(//,5X,'ELEMENT',1X,I3,//,6(5X,F7.4))
   50 RETURN
      END
```

```
      SUBROUTINE TEMP
      PARAMETER N=6,M=3,NN=242,NPOIN=121,NELEM=200
      COMMON/INP/NOD(NELEM,N),X(NPOIN),Y(NPOIN),NPT(NN),NMP(NN),VAL(NN
      COMMON/INP2/IPLOT,IPRINT,LIN,NEUMN,NPRES,T,H(10),NH,HA,KCALL
      COMMON/SYST/A(M),B(M),C(M),DELTA
      COMMON/EL2/HX(M),U(M)
      COMMON/ELEMT/STE(NELEM,N,N),SM(NN,NN),RR(NELEM,N),R(NN)
      COMMON/SYST2/BB(NELEM,M),CC(NELEM,M),DEL(NELEM),AA(NELEM,M)
      DIMENSION TM(NPOIN,NPOIN),RHS(NPOIN)
      DIMENSION WKAREA(NPOIN)
C
C     CALCULATE SYSTEM MATRIX FOR TEMPERATURE FIELD
C
      CALL SMATR
      DO 2 I=1,NPOIN
      DO 1 J=1,NPOIN
    1 TM(I,J)=SM(I,J)
    2 RHS(I)=R(I)
      CALL LEQT1F(TM,1,NPOIN,NPOIN,RHS,0,WKAREA,IER)
      WRITE(6,10)
      WRITE(6,20) (I,RHS(I),I=1,NPOIN)
      RETURN
   10 FORMAT(1H1,//,10X,,TEMPERATURE,,//,1X,13H NODE    VALUE,3(19H
     1NODE    VALUE ))
   20 FORMAT((1X,I3,E12.5,3(I6,E12.5)))
      END




      SUBROUTINE TELM(I)
      PARAMETER N=6,M=3,NN=242,NPOIN=121,NELEM=200
      COMMON/ELEMT/STE(NELEM,N,N),SM(NN,NN),RR(NELEM,N),R(NN)
      COMMON/EL2/HX(M),U(M)
      COMMON/SYST/A(M),B(M),C(M),DELTA
C
C     CALCULATES ELEMENT MATRICES FOR TEMPFRATURE
C
      DO 10 J=1,3
      RR(I,J)=0.
      DO 10 K=1,3
      STE(I,J,K)=(C(J)*C(K)+B(J)*B(K))/(4.0*DELTA)
   10 CONTINUE
      DO 47 J=1,M
      DO 46 K=1,M
      DO 46 L=1,M
   46 RR(I,J)=RR(I,J)+(C(L)*C(K)+B(L)*B(K))*(HX(L)*HX(K)+U(L)*U(K))
   47 RR(I,J)=RR(I,J)/(12.*DELTA)
      RETURN
      END
```

```
      SUBROUTINE OUTPUT
      PARAMETER N=6,M=3,NN=242,NPOIN=121,NELEM=200
      COMMON/ELEMT/STE(NELEM,N,N),SM(NN,NN),RR(NELEM,N),R(NN)
      COMMON/INP2/IPLOT,IPRINT,LIN,NEUMN,NPRES,T,H(10),NH,HA,KCALL
      COMMON/PLT/VEL(20,20),MAG(20,20)
      REAL MAG
C
C     PRINTS OUT THE RESULTS
C
      IF(IPLOT.EQ.0) GO TO 5
      READ(5,60) N1,N2
    5 CONTINUE
      WRITE(6,10)
      WRITE(6,70) HA,T
      WRITE(6,50)
      WRITE(6,20)
      WRITE(6,30) (I,R(I),I=1,NPOIN)
      WRITE(6,40)
      WRITE(6,20)
      WRITE(6,30) (I-NPOIN,R(I),I=NPOIN+1,NN)
      IF(IPLOT.EQ.0) GO TO 6
      DO 1 J=1,N2
      L=N2-J+1
      DO 1 I=1,N1
      K=(J-1)*N1+I
      MAG(I,L)=R(K)
    1 VEL(I,L)=R(K+NPOIN)
   10 FORMAT(1H1,///,10X,'SOLUTION BY FINITE ELEMENTS',/)
   20 FORMAT(/,1X,13H NODE   VALUE,3(19H       NODE   VALUE ))
   30 FORMAT((1X,I3,E12.5,3(I6,E12.5)))
   40 FORMAT(//,10X,'VELOCITY',/)
   50 FORMAT(//,10X,'MAGNETIC INTENSITY',/)
   60 FORMAT(2I3)
   70 FORMAT(9X,'HA',9X,'T',/,8X,F7.4,4X,F3.1)
      END
```

Sample Input / Output

In preparing input data to computer program, the domain is to be discretized into elements and numbered. An example of triangularization is given below:

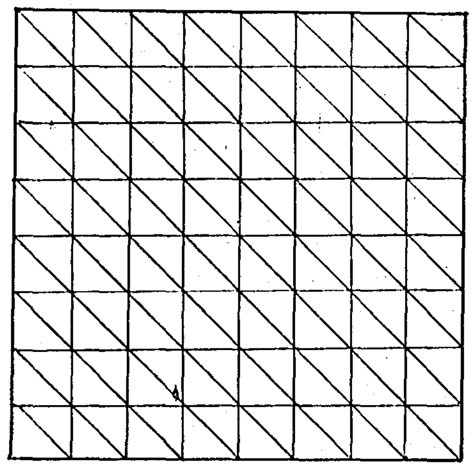

Fig. 35. Finite Element Mesh Structure

Following is input formats and a sample input/output for the mesh structure of Fig. 35, for the two - dimensional computer program:

Variable	Format
HEADG	80 A1
NDIM, LIN, ITEMP, IPLOT, IPRINT, NEUMN, NPRES	7 I5
NH, T, H (I)	I3, F7.3, 10F5.2
K, NOD (I, J)	24I3
Y (I), X(I)	22F3-1
NPT (I), VAL (I)	7 (I3, F7.2)
NMP (I)	16I5

FOLLOWING IS THE INPUT TO FEM PROGRAM FOR

SQUARE DUCT WITH CONDUCTING WALLS***

NUMBER OF NODES 81
NUMBER OF ELEMENTS 128

2 1 1 0 0 1 32

X AND Y COORDINATES

NODE	X	Y	NODE	X	Y	NODE	X	Y
1	-1.00	1.00	2	-.75	1.00	3	-.50	1.00
4	-.25	1.00	5	.00	1.00	6	.25	1.00
7	.50	1.00	8	.75	1.00	9	1.00	1.00
10	-1.00	.75	11	-.75	.75	12	-.50	.75
13	-.25	.75	14	.00	.75	15	.25	.75
16	.50	.75	17	.75	.75	18	1.00	.75
19	-1.00	.50	20	-.75	.50	21	-.50	.50
22	-.25	.50	23	.00	.50	24	.25	.50
25	.50	.50	26	.75	.50	27	1.00	.50
28	-1.00	.25	29	-.75	.25	30	-.50	.25
31	-.25	.25	32	.00	.25	33	.25	.25
34	.50	.25	35	.75	.25	36	1.00	.25
37	-1.00	.00	38	-.75	.00	39	-.50	.00
40	-.25	.00	41	.00	.00	42	.25	.00
43	.50	.00	44	.75	.00	45	1.00	.00
46	-1.00	-.25	47	-.75	-.25	48	-.50	-.25
49	-.25	-.25	50	.00	-.25	51	.25	-.25
52	.50	-.25	53	.75	-.25	54	1.00	-.25
55	-1.00	-.50	56	-.75	-.50	57	-.50	-.50
58	-.25	-.50	59	.00	-.50	60	.25	-.50
61	.50	-.50	62	.75	-.50	63	1.00	-.50
64	-1.00	-.75	65	-.75	-.75	66	-.50	-.75
67	-.25	-.75	68	.00	-.75	69	.25	-.75
70	.50	-.75	71	.75	-.75	72	1.00	-.75
73	-1.00	-1.00	74	-.75	-1.00	75	-.50	-1.00
76	-.25	-1.00	77	.00	-1.00	78	.25	-1.00
79	.50	-1.00	80	.75	-1.00	81	1.00	-1.00

THE ELEMENTS AND THEIR NODES

ELEM	I	J	M	ELEM	I	J	M	ELEM	I	J	M	ELEM	I	J	M
1	2	1	10	2	2	10	11	3	3	2	11	4	3	11	12
5	4	3	12	6	4	12	13	7	5	4	13	8	5	13	14
9	6	5	14	10	6	14	15	11	7	6	15	12	7	15	16
13	8	7	16	14	8	16	17	15	9	8	17	16	9	17	18
17	11	10	19	18	11	19	20	19	12	11	20	20	12	20	21
21	13	12	21	22	13	21	22	23	14	13	22	24	14	22	23
25	15	14	23	26	15	23	24	27	16	15	24	28	16	24	25
29	17	16	25	30	17	25	26	31	18	17	26	32	18	26	27
33	20	19	28	34	20	28	29	35	21	20	29	36	21	29	30
37	22	21	30	38	22	30	31	39	23	22	31	40	23	31	32
41	24	23	32	42	24	32	33	43	25	24	33	44	25	33	34
45	26	25	34	46	26	34	35	47	27	26	35	48	27	35	36
49	29	28	37	50	29	37	38	51	30	29	38	52	30	38	39
53	31	30	39	54	31	39	40	55	32	31	40	56	32	40	41
57	33	32	41	58	33	41	42	59	34	33	42	60	34	42	43
61	35	34	43	62	35	43	44	63	36	35	44	64	36	44	45
65	38	37	46	66	38	46	47	67	39	38	47	68	39	47	48
69	40	39	48	70	40	48	49	71	41	40	49	72	41	49	50
73	42	41	50	74	42	50	51	75	43	42	51	76	43	51	52
77	44	43	52	78	44	52	53	79	45	44	53	80	45	53	54
81	47	46	55	82	47	55	56	83	48	47	56	84	48	56	57
85	49	48	57	86	49	57	58	87	50	49	58	88	50	58	59
89	51	50	59	90	51	59	60	91	52	51	60	92	52	60	61
93	53	52	61	94	53	61	62	95	54	53	62	96	54	62	63
97	56	55	64	98	56	64	65	99	57	56	65	100	57	65	66
101	58	57	66	102	58	66	67	103	59	58	67	104	59	67	68
105	60	59	68	106	60	68	69	107	61	60	69	108	61	69	70
109	62	61	70	110	62	70	71	111	63	62	71	112	63	71	72
113	65	64	73	114	65	73	74	115	66	65	74	116	66	74	75
117	67	66	75	118	67	75	76	119	68	67	76	120	68	76	77
121	69	68	77	122	69	77	78	123	70	69	78	124	70	78	79
125	71	70	79	126	71	79	80	127	72	71	80	128	72	80	81

NODES WITH PRESCRIBED VALUES

NODE	VALUE	NODE	VALUE	NODE	VALUE	NODE	VALUE
82	.000	83	.000	84	.000	85	.000
86	.000	87	.000	88	.000	89	.000
90	.000	91	.000	99	.000	100	.000
108	.000	109	.000	117	.000	118	.000
126	.000	127	.000	135	.000	136	.000
144	.000	145	.000	153	.000	154	.000
162	.000	155	.000	156	.000	157	.000
158	.000	159	.000	160	.000	161	.000

SOLUTION BY FINITE ELEMENTS

HA	T
5.0000	1.0

MAGNETIC INTENSITY

NODE	VALUE	NODE	VALUE	NODE	VALUE	NODE	VALUE
1	-.11769+000	2	-.12654+000	3	-.14003+000	4	-.14929+000
5	-.15261+000	6	-.15003+000	7	-.14221+000	8	-.13128+000
9	-.12410+000	10	-.10863+000	11	-.11467+000	12	-.12431+000
13	-.13156+000	14	-.13415+000	15	-.13160+000	16	-.12427+000
17	-.11416+000	18	-.10795+000	19	-.78727-001	20	-.81542-001
21	-.87121-001	22	-.91759-001	23	-.93464-001	24	-.91660-001
25	-.86777-001	26	-.86759-001	27	-.77602-001	28	-.41630-001
29	-.42739-001	30	-.45189-001	31	-.47331-001	32	-.48100-001
33	-.47136-001	34	-.44730-001	35	-.42023-001	36	-.40792-001
37	-.22814-002	38	-.22553-002	39	-.21640-002	40	-.20317-002
41	-.19132-002	42	-.17946-002	43	-.16623-002	44	-.15710-002
45	-.15449-002	46	.35966-001	47	.38196-001	48	.40903-001
49	.43309-001	50	.44274-001	51	.43505-001	52	.41353-001
53	.38912-001	54	.57804-001	55	.73776-001	56	.76913-001
57	.82951-001	58	.87534-001	59	.89636-001	60	.87928-001
61	.83294-001	62	.77715-001	63	.74901-001	64	.10412+000
65	.11033+000	66	.12045+000	67	.12777+000	68	.13033+000
69	.12773+000	70	.12048+000	71	.11684+000	72	.10500+000
73	.12028+000	74	.12746+000	75	.13839+000	76	.14621+000
77	.14878+000	78	.14548+000	79	.13621+000	80	.12272+000
81	.11386+000						

VELOCITY

NODE	VALUE	NODE	VALUE	NODE	VALUE	NODE	VALUE
1	.00000	2	.00000	3	.00000	4	.00000
5	.00000	6	.00000	7	.00000	8	.00000
9	.00000	10	.00000	11	.22943-001	12	.31348-001
13	.34001-001	14	.34365-001	15	.33355-001	16	.30111-001
17	.21542-001	18	.00000	19	.00000	20	.26224-001
21	.38592-001	22	.43354-001	23	.44380-001	24	.42981-001
25	.38031-001	26	.25794-001	27	.00000	28	.00000
29	.26307-001	30	.40283-001	31	.46253-001	32	.47750-001
33	.46112-001	34	.40120-001	35	.26244-001	36	.00000
37	.00000	38	.26189-001	39	.40569-001	40	.46922-001
41	.48616-001	42	.46922-001	43	.40569-001	44	.26189-001
45	.00000	46	.00000	47	.26244-001	48	.40120-001
49	.46112-001	50	.47750-001	51	.46253-001	52	.40283-001
53	.26307-001	54	.00000	55	.00000	56	.25794-001
57	.38031-001	58	.42981-001	59	.44380-001	60	.43354-001
61	.38592-001	62	.26224-001	63	.00000	64	.00000
65	.21542-001	66	.30111-001	67	.33355-001	68	.34365-001
69	.34001-001	70	.31348-001	71	.22943-001	72	.00000
73	.00000	74	.00000	75	.00000	76	.00000
77	.00000	78	.00000	79	.00000	80	.00000
81	.00000						

TEMPERATURE

NODE	VALUE	NODE	VALUE	NODE	VALUE	NODE	VALUE
1	.00000	2	.00000	3	.00000	4	.00000
5	.00000	6	.00000	7	.00000	8	.00000
9	.00000	10	.00000	11	.19133-002	12	.30840-002
13	.37525-002	14	.39713-002	15	.37480-002	16	.30599-002
17	.18615-002	18	.00000	19	.00000	20	.32338-002
21	.52327-002	22	.63832-002	23	.67649-002	24	.63816-002
25	.52157-002	26	.32015-002	27	.00000	28	.00000
29	.40132-002	30	.65151-002	31	.79545-002	32	.84321-002
33	.79524-002	34	.65040-002	35	.39976-002	36	.00000
37	.00000	38	.42610-002	39	.69301-002	40	.84678-002
41	.89777-002	42	.84678-002	43	.69301-002	44	.42610-002
45	.00000	46	.00000	47	.39976-002	48	.65040-002
49	.79524-002	50	.84321-002	51	.79545-002	52	.65151-002
53	.40132-002	54	.00000	55	.00000	56	.32015-002
57	.52157-002	58	.63816-002	59	.67649-002	60	.63831-002
61	.52327-002	62	.32338-002	63	.00000	64	.00000
65	.18615-002	66	.30599-002	67	.37480-002	68	.39713-002
69	.37525-002	70	.30840-002	71	.19133-002	72	.00000
73	.00000	74	.00000	75	.00000	76	.00000
77	.00000	78	.00000	79	.00000	80	.00000
81	.00000						